QED corrections in $\bar{B} \to \bar{K}\ell^+\ell^-$: comparing PHOTOS to a Monte Carlo based on a fully differential NLO computation.

QED in weak decays Workshop

Davide Lancierini, University of Zürich

23.06.2022

Outline

- Introduction on Bremsstrahlung and Final State Radiation (FSR)
  - What is Bremsstrahlung, what does it depend on
- [PHOTOS] vs our Monte Carlo for FSR simulation
  - How does PHOTOS work? How does our MC work?
  - Kinematic distributions of decay products
  - Comparisons between [PHOTOS] and our MC, with and without resonant J/ψ contribution
- How does bremsstrahlung recovery affect our measurements
- Conclusions

Bremsstrahlung

- Bremsstrahlung effects arise from the interaction of charged particles with the detector material (Coulomb field of atoms)
- Probability $\propto E/m^2$ $\rightarrow$ mainly affects electrons
- An electron loses energy by bremsstrahlung at a rate dE/dx nearly proportional to its energy
  $\rightarrow$ fractional loss is roughly independent of $e^{\pm}$ energy .

PDG

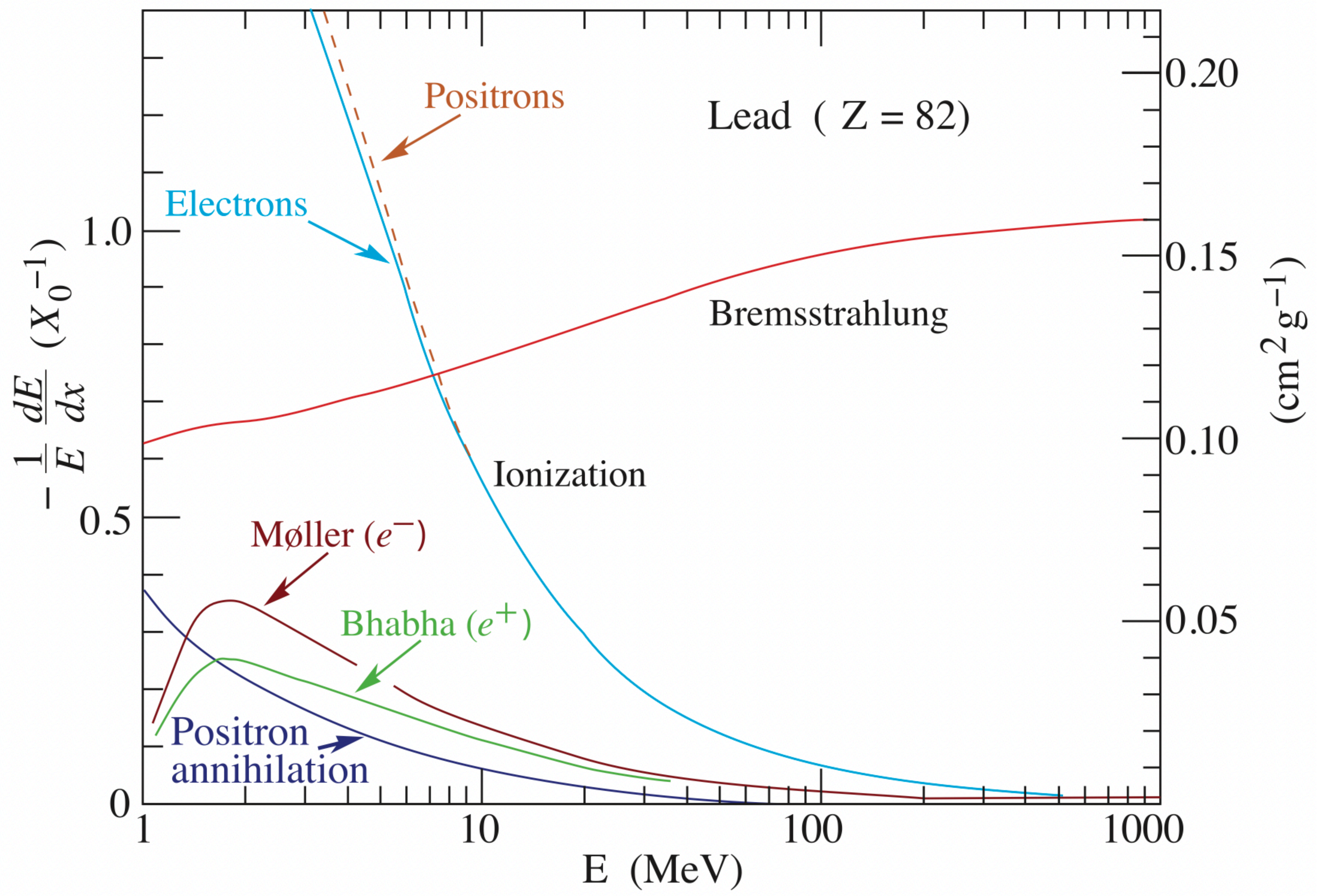

The LHCb detector

- 9fb^{-1} integrated luminosity collected at $7-8-13\,\text{TeV}$ pp collisions, $3\times10^{32}\text{cm}^{-2}\text{s}^{-1}$ instantaneous lumi

- Forward arm spectrometer designed for heavy flavour physics
- Instrumented in the forward region where $\sigma(pp\to b\bar{b}X)$ is maximal
- Low-p_T triggers (few GeV)
- Excellent vertexing (VELO) and PID capabilities to identify displaced $b-$hadron vertices and rare decays
- Momentum measurement with spectrometer $\sigma_p/p\sim0.5\,\%$

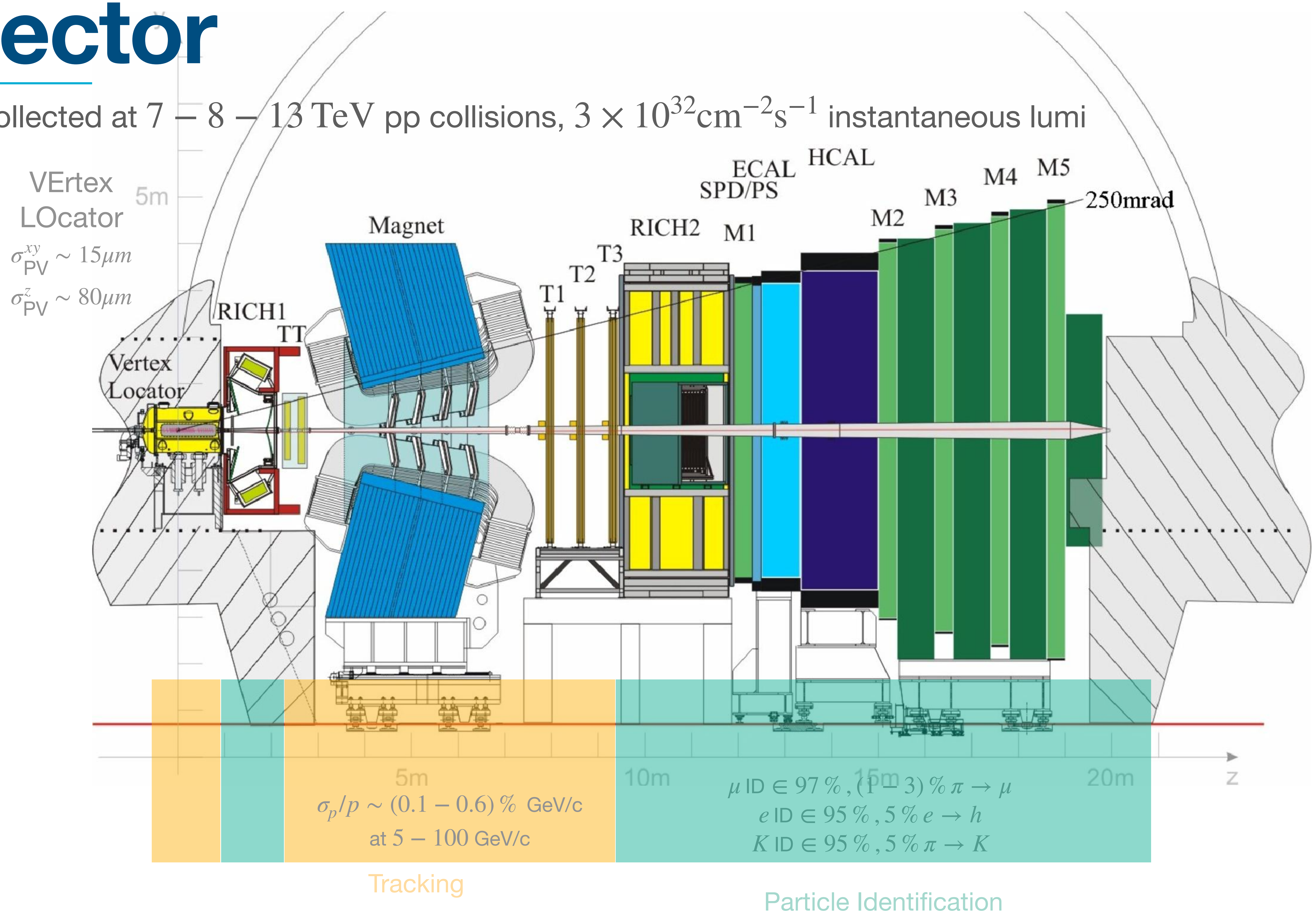

Brem photons emitted at LHCb

- Most brem emission is due to material interaction and occurs before the bending magnet

- If brem is emitted before the bending magnet, momentum resolution is affected

- For $E(e^{\pm}) > 10$ GeV, average number of brem photons emitted per electron, before the magnet, given $\min(E_T(\gamma)) = 75$ MeV is $\simeq 1$

- Brem recovery algorithm in place to add back lost momentum to the electron tracks (more on this later)

Plot credits @ M. Borsato

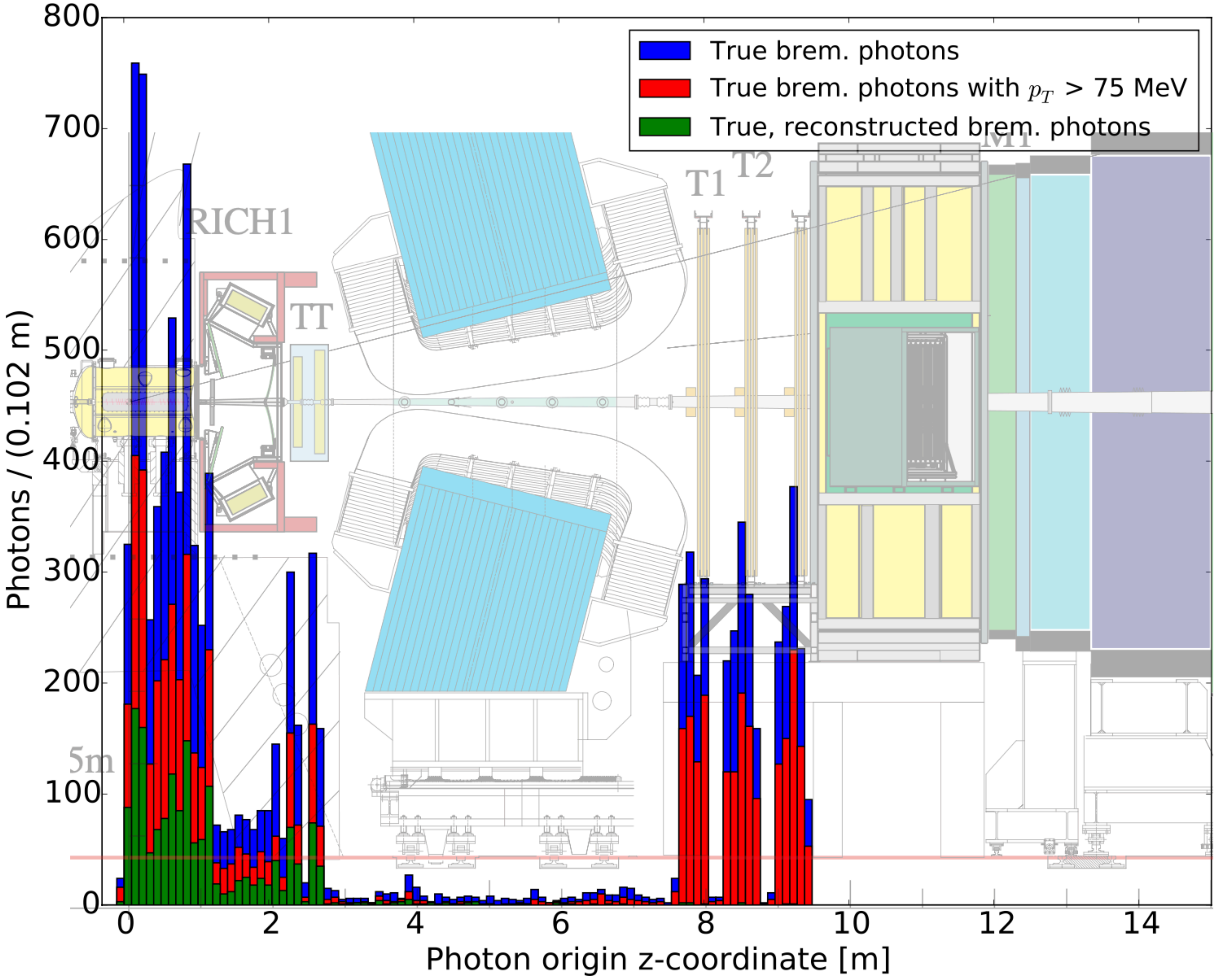

Final State Radiation (FSR)

- Energy radiated through photon emission from charged final state particles in B-meson decays

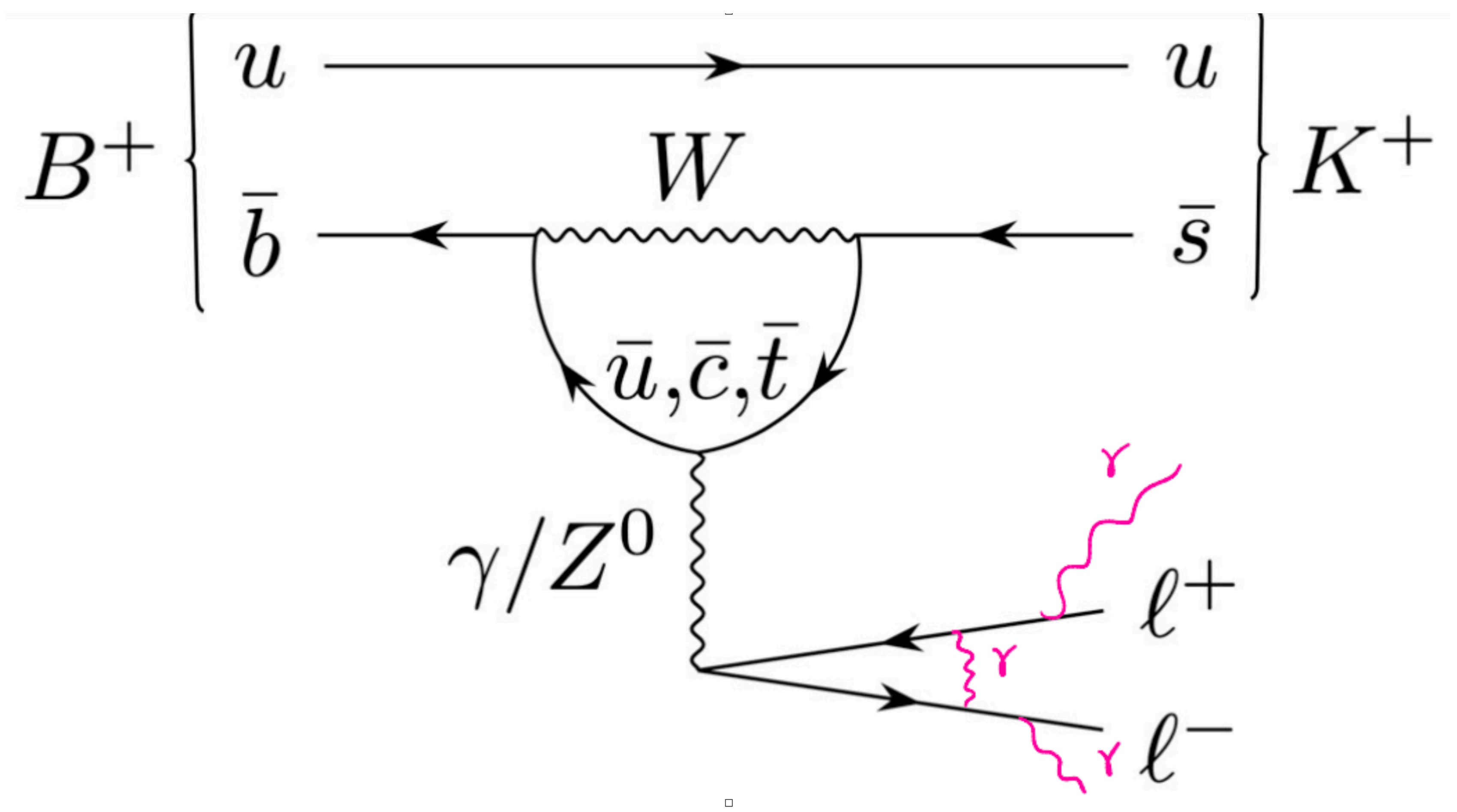

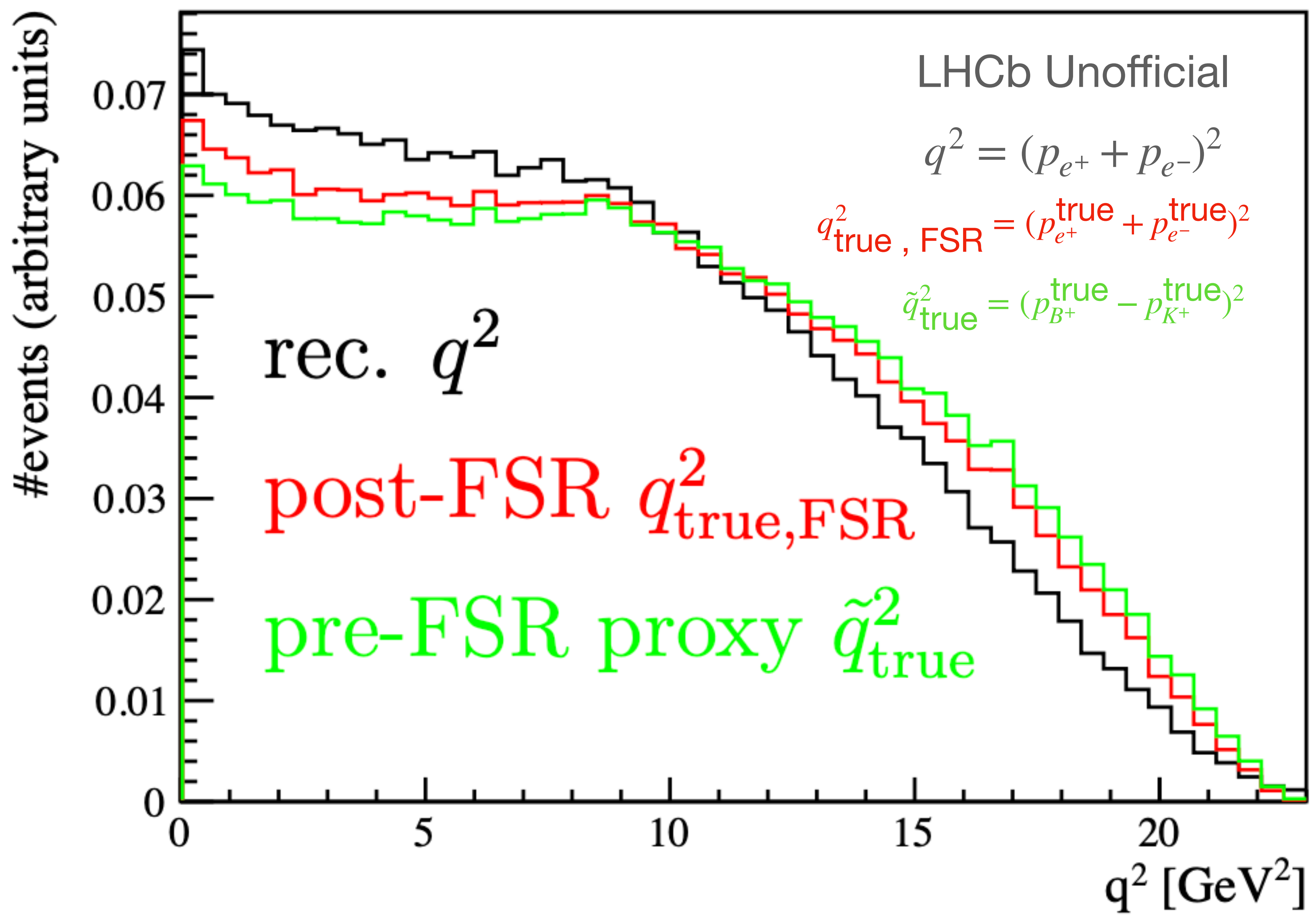

- This effect has to be taken into account in order to correctly model the distributions on which the detection efficiencies depend on

PHOTOS

https://arxiv.org/pdf/1011.0937.pdf

- How is this accounted for in LHCb? Via the [PHOTOS] package
- [PHOTOS] corrects a MC event after it has been fully generated to account for FSR, at the generator level, i.e. prior to any detector effect
- Interface with [PHOTOS] in LHCb simulation is via the [EvtGen] package which handles the decay of heavy flavour hadrons

$$d\sigma^{Born}(a^0 \to \ell^\pm b^0) = |M_{Born}|\underbrace{d\phi_2(a^0;\ell^\pm,b^0)}_{cos\theta_l,q^2}$$

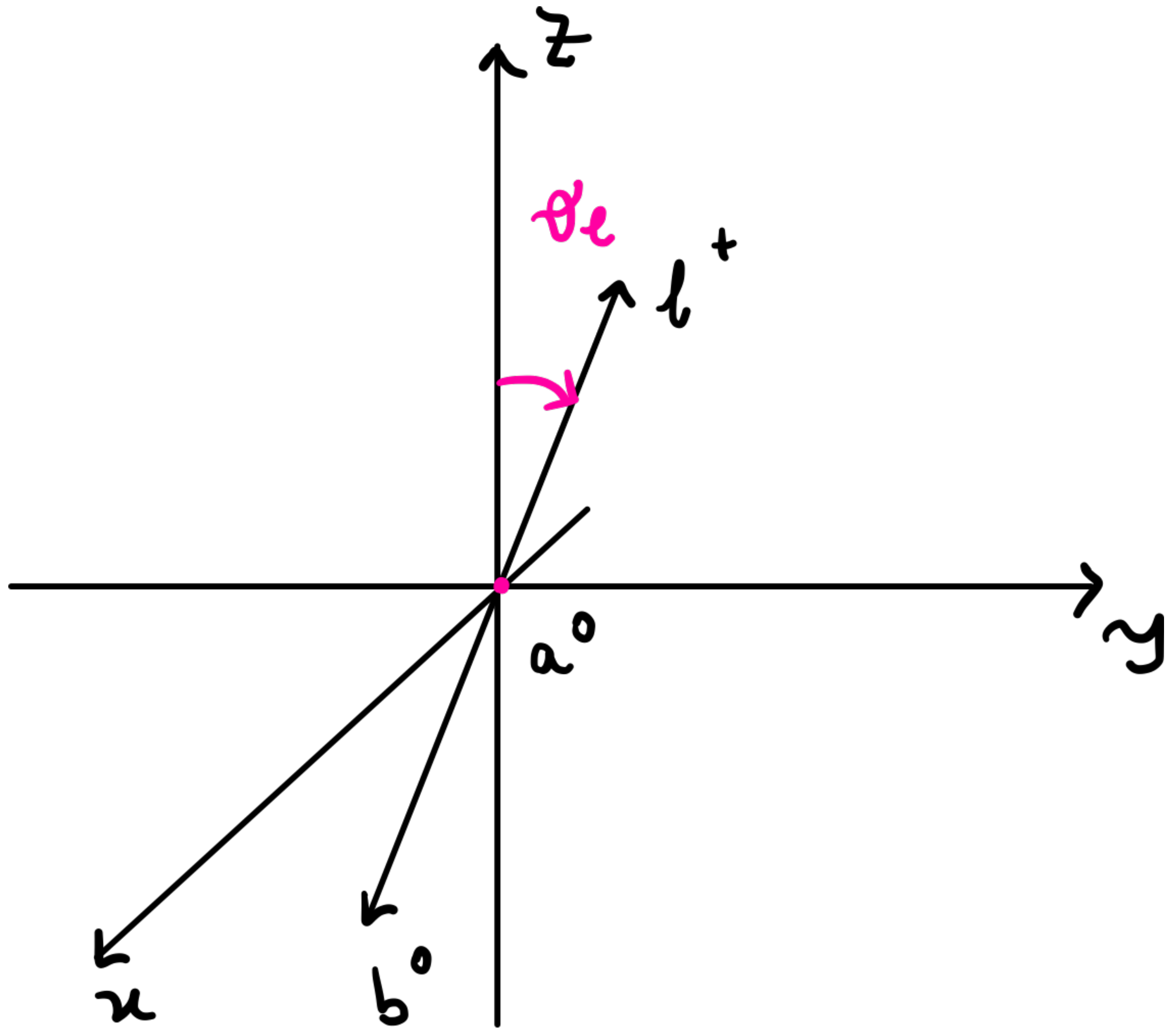

PHOTOS

https://arxiv.org/pdf/1011.0937.pdf

- How is this accounted for in LHCb? Via the [PHOTOS] package
- [PHOTOS] corrects a MC event after it has been fully generated to account for FSR, at the generator level, i.e. prior to any detector effect
- Interface with [PHOTOS] in LHCb simulation is via the [EvtGen] package which handles the decay of heavy flavour hadrons

$$d\sigma^{Born}(a^0 \to \ell^{\pm} b^0) = |M_{Born}| \underbrace{d\phi_2(a^0; \ell^{\pm}, b^0)}_{cos\theta_l, q^2}$$

$$\Downarrow$$

$$d\sigma^{NLO}(a^0 \to (\ell^{\pm}\gamma) b^0) = |M_{NLO}| \underbrace{d\phi_3(a^0; \ell^{\pm}, \gamma, b^0)}_{cos\theta_\ell, q^2, cos\theta_\gamma, \phi_\gamma, E_\gamma}$$

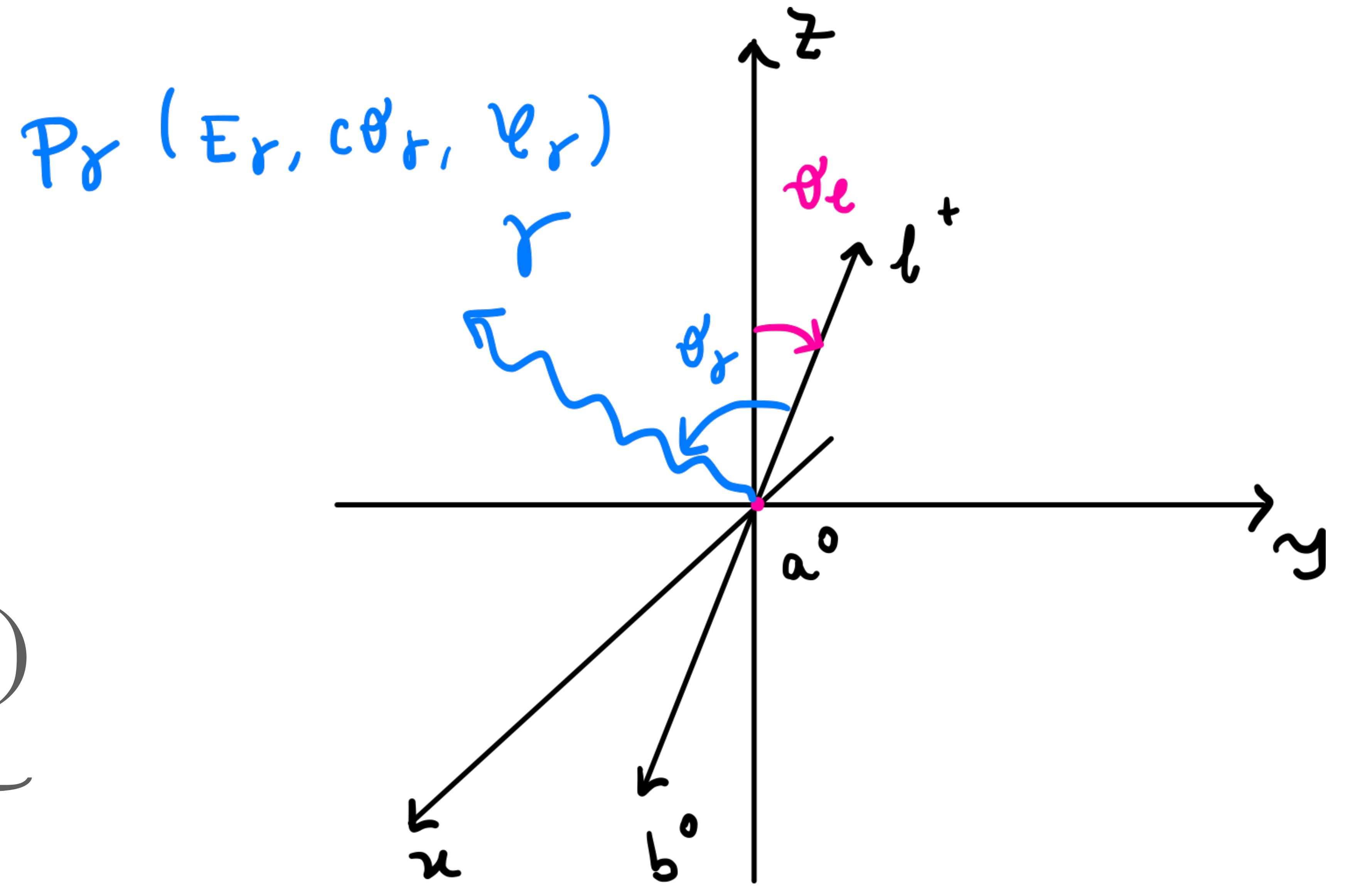

PHOTOS

https://arxiv.org/pdf/1011.0937.pdf

- Assuming factorisation of splitting function in leading log approximation

$$|M_{NLO}|^2 = |M_{Born}|^2 f_{brem}(E_\gamma, cos\theta_\gamma, \phi_\gamma)$$

$$\Downarrow$$

$$d\sigma^{NLO}(a^0 \to (\ell^\pm \gamma) b^0) = d\sigma^{Born}(a^0 \to \ell^\pm b^0) d\phi_3 f_{brem}(E_\gamma, cos\theta_\gamma, \phi_\gamma)$$

- f_{brem}'s functional form depends on properties of the charged particle and determines probability of brem. photon emission.

- Once the photon is generated, it is added to the event which is modified accordingly

Our Monte Carlo setup: framework

- Our recent work [2205.08635] aims at testing the approximations adopted by [PHOTOS] by implementing the fully differential results presented in [2009.00929]

- This results confirms the predictions of [1605.07633] and extends it by building a custom Monte Carlo event generator.

$$\bar{B}(p_B) \to \bar{K}(p_K)\ell^+(p_1)\ell^-(p_2) + \gamma(k)$$

- $q - RF$

$$q^2 = (p_1 + p_2)^2$$

$$c_\ell = -\left(\frac{\vec{p}_1 \cdot \vec{p}_K}{|\vec{p}_1||\vec{p}_K|}\right)_{q-RF}$$

- $q_0 - RF$

$$q_0^2 = (p_B - p_K)^2$$

$$c_0 = -\left(\frac{\vec{p}_1 \cdot \vec{p}_K}{|\vec{p}_1||\vec{p}_K|}\right)_{q_0-RF}$$

$$\bar{p}_B = p_B - k = p_1 + p_2 + p_K, \qquad \bar{p}_B^2 = (m_B^{rec})^2$$

Our Monte Carlo setup: framework

- Our recent work [2205.08635] aims at testing the approximations adopted by [PHOTOS] by implementing the fully differential results presented in [2009.00929]

- This results confirms the predictions of [1605.07633] and extends it by building a custom Monte Carlo event generator.

$$\mathcal{A}_{\bar{B}\to\bar{K}\ell^+\ell^-} \equiv \langle \bar{K}\ell^+\ell^- | (-\mathcal{L}_{\rm int}) | \bar{B} \rangle = \frac{G_F}{\sqrt{2}} V^*_{\rm ts} V_{\rm tb}\, L_0 \cdot H_0 + \mathcal{O}(\alpha)$$

$$\begin{aligned} L_0^\mu(q^2) &= \bar{u}(\ell^-)\gamma^\mu(C_V + C_A\gamma_5)v(\ell^+)\,, \\ H_0^\mu(q^2) &= f_+(q^2)(p_B + p_K)^\mu + f_-(q^2)(p_B - p_K)^\mu \end{aligned}$$

Our Monte Carlo setup: framework

- Set $E_{\gamma,cut}(= 100$ KeV) so that events with $E_\gamma \lessgtr E_{\gamma,cut}$ can be simulated using a 3 or 4 body matrix element and phase space.

- The relative normalisation between 3 body and 4 body events is a key theory input:

$$f^{th}(E_{\gamma,cut}) \equiv \frac{N_3}{N_4} = \frac{\Gamma_3}{\Gamma_4}$$

- By observing that the total rate $\Gamma_{tot} \equiv \Gamma_3 + \Gamma_4 = \Gamma_{tree} \times [1 + \mathcal{O}(\alpha)]$ one can easily obtain a relation for $f^{th}(E_{\gamma,cut})$

$$f^{th}(E_{\gamma,cut}) = \left(\frac{\Gamma_{tree}}{\Gamma_3} - 1\right)^{-1}$$

Our Monte Carlo results: only rare mode

- The 3 and 4 body events are simulated separately using the hit-or-miss algorithm provided by the [zfit package]

3 body (includes virtual + soft contribution)

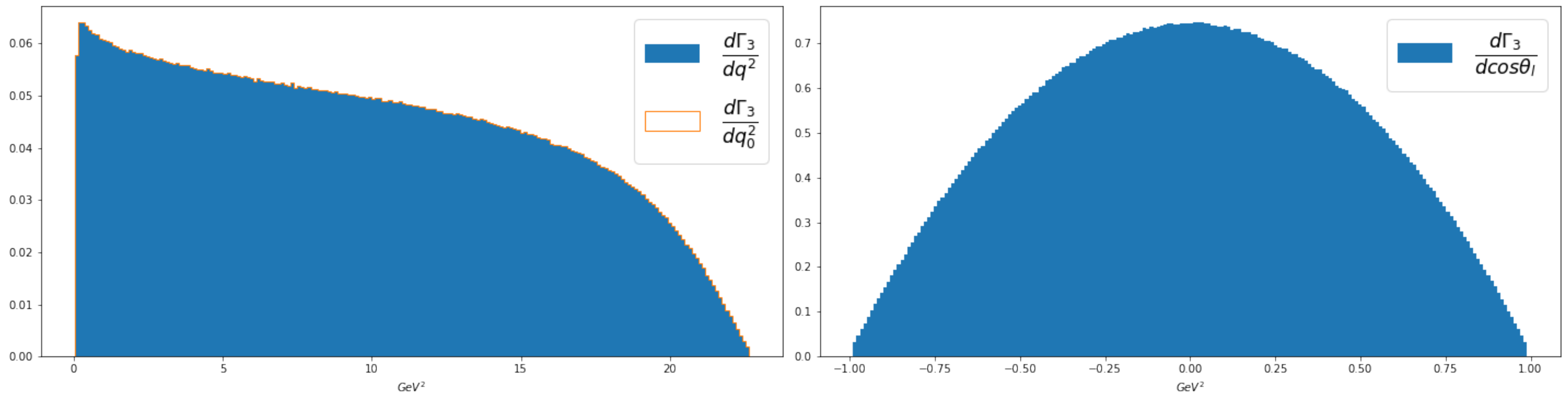

4 body (real emission)

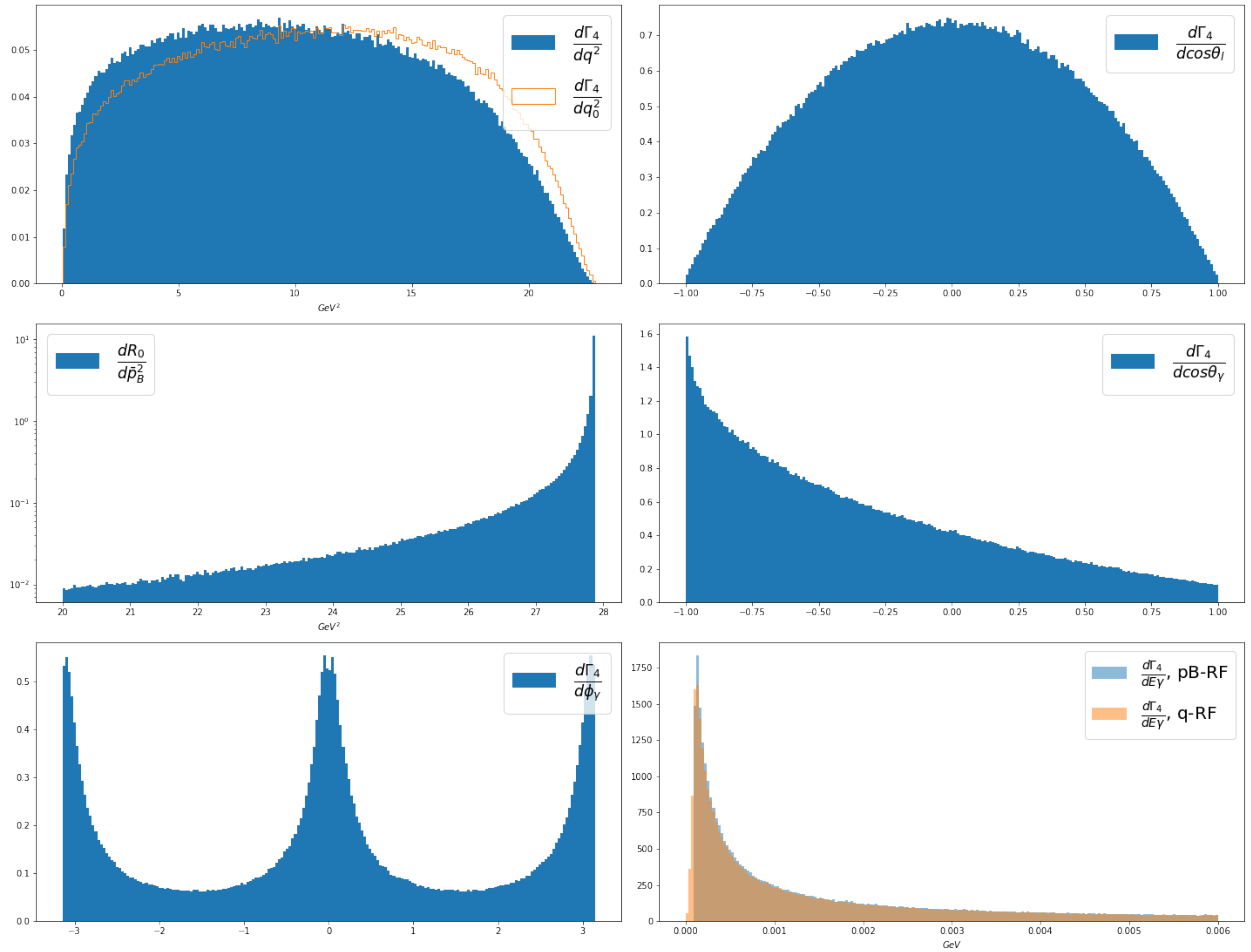

Rare mode:

Experimentalists (only?) jargon to indicate non resonant

$$\bar{B} \to \bar{K}\ell^+\ell^-$$

Our Monte Carlo results: only rare mode

- The 3 and 4 body events are simulated separately using the hit-or-miss algorithm provided by the [zfit package]

3 body (includes virtual + soft contribution)

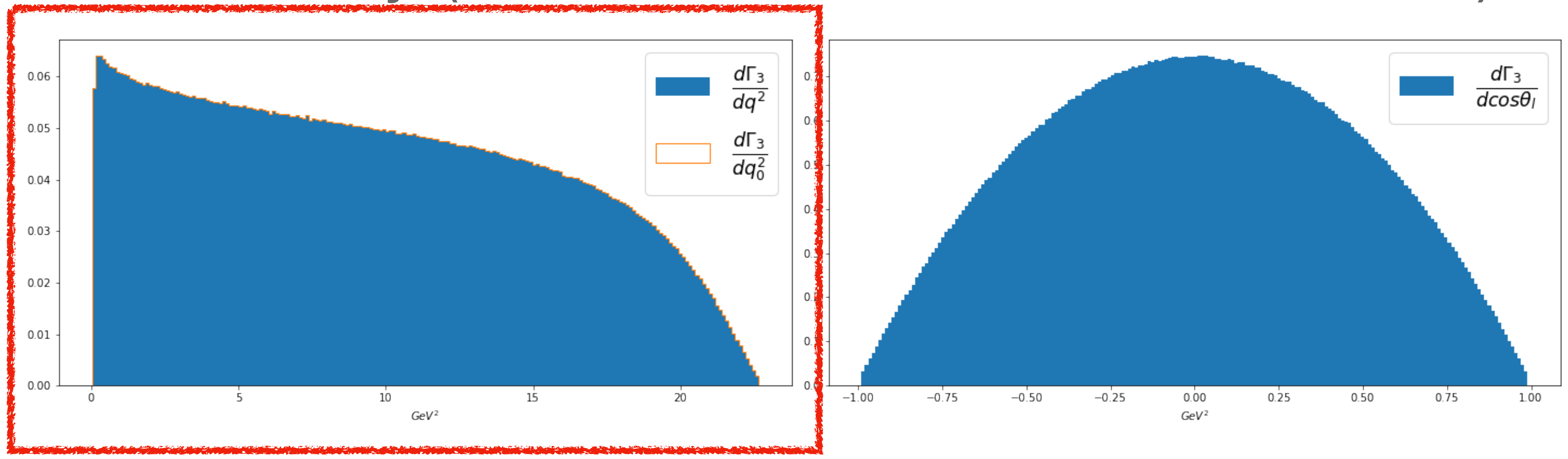

$$q_0^2 = q_2 \quad \text{for a 3 body decay}$$

4 body (real emission)

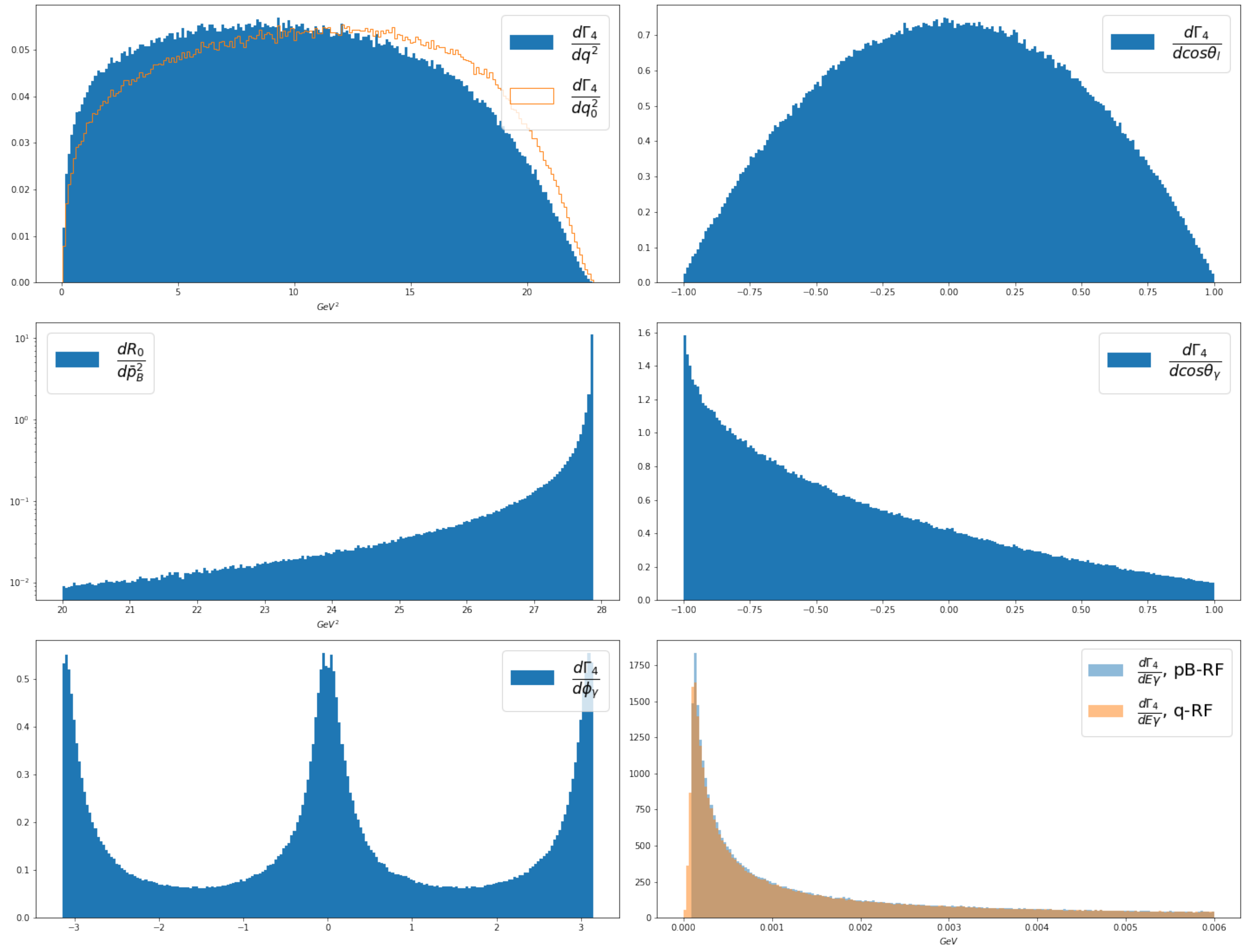

Our Monte Carlo results: only rare mode

- The 3 and 4 body events are simulated separately using the hit-or-miss algorithm provided by the [zfit package]

$q_0^2 \neq q_2$ for the 4 body decay,

4 body (real emission)

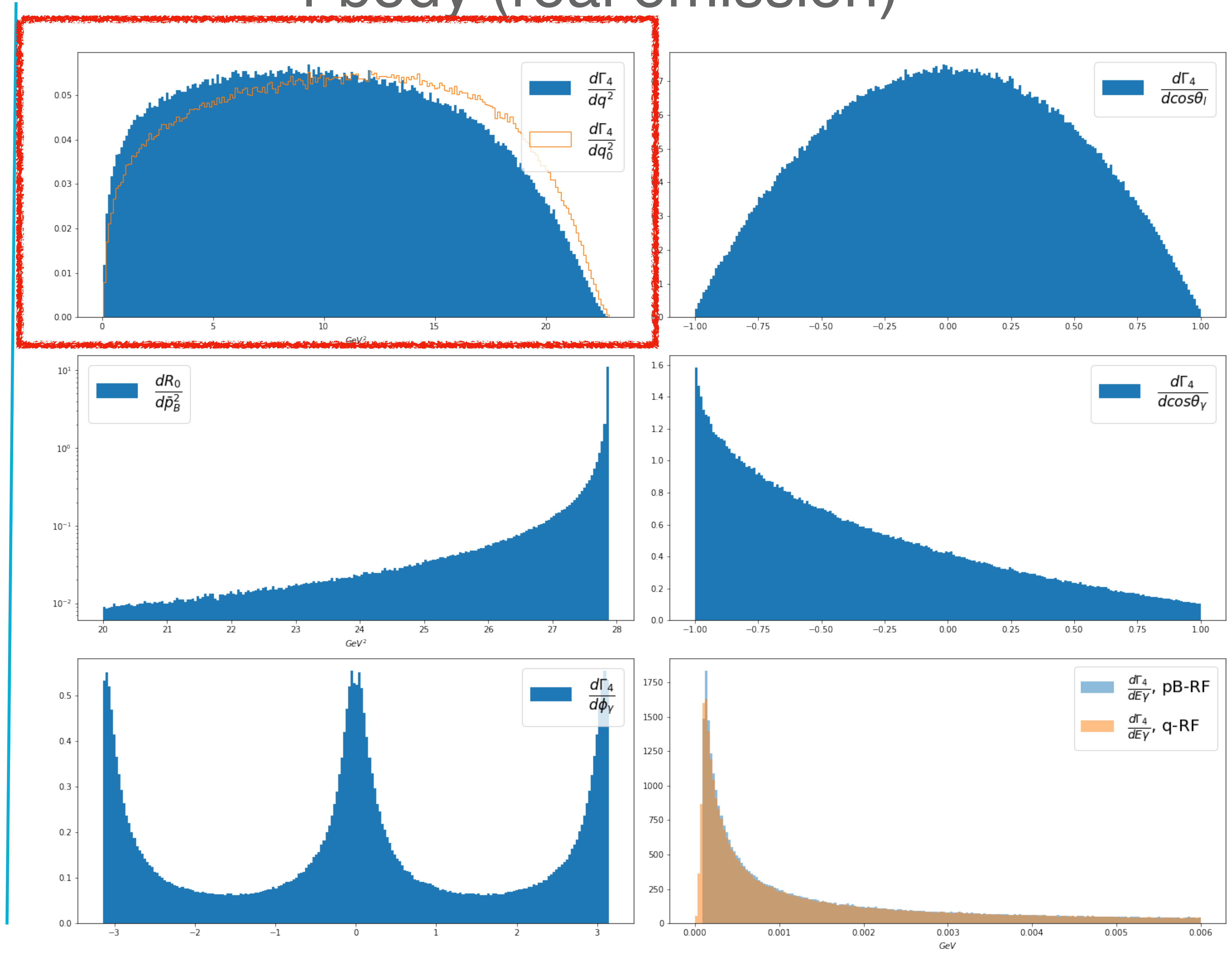

Our Monte Carlo results: only rare mode

- The 3 and 4 body events are simulated separately using the hit-or-miss algorithm provided by the [zfit package]

$q_0^2 \neq q_2$ for the 4 body decay,

different efficiency of
$1.1 < q_2/\mathrm{GeV}^2 < 6$ & $\bar{p}_B^2 > (m_B^{rec})^2$
cut in μ/e impacts on value of QED corrections on LFU ratios

4 body (real emission)

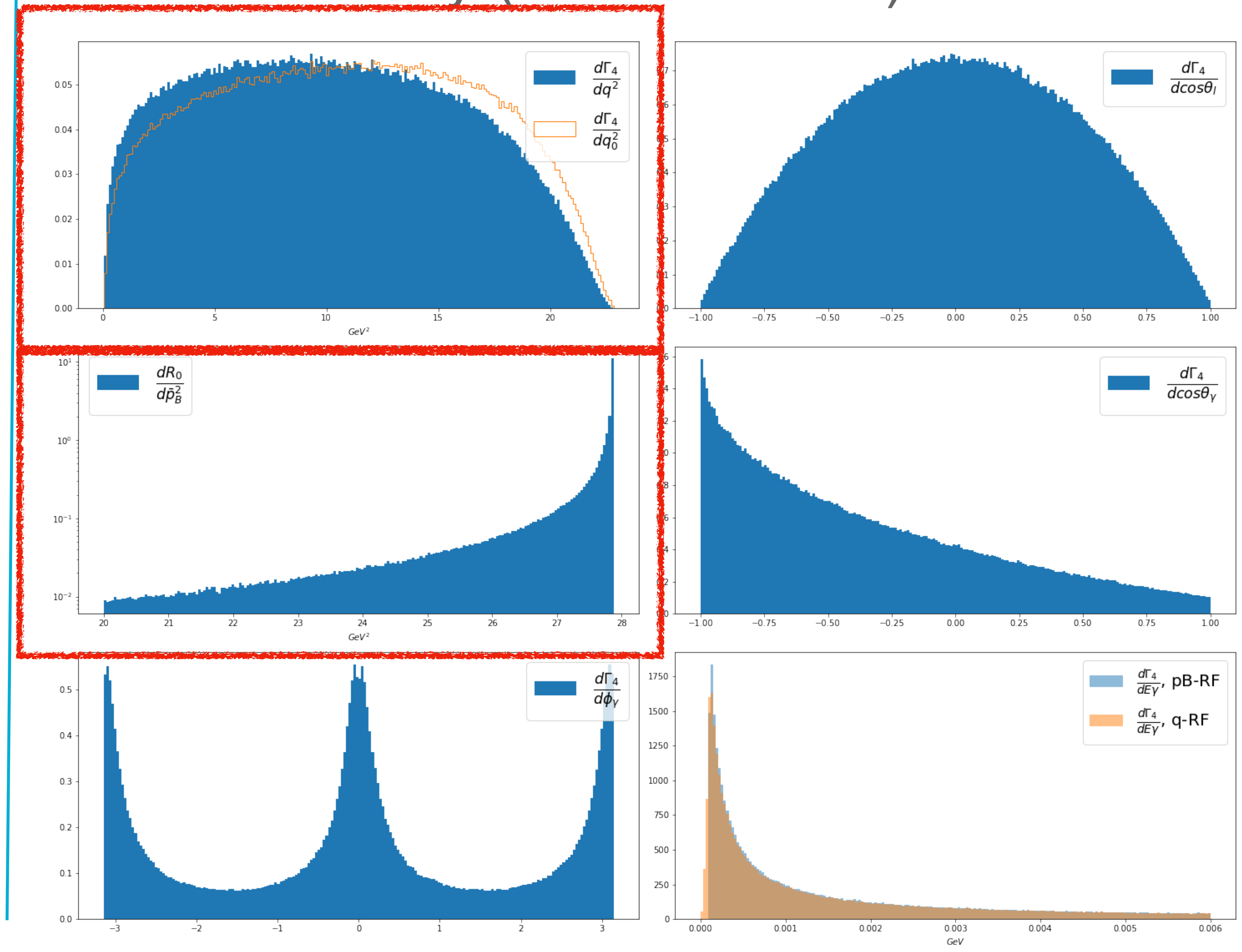

Our Monte Carlo results: only rare mode

- These sets of 3 and 4 body decays are merged using a proportion given by $f^{th}(E_{\gamma,cut}) \rightarrow$ obtaining a NLO "tuple" which contains all the kinematic details of the daughters.

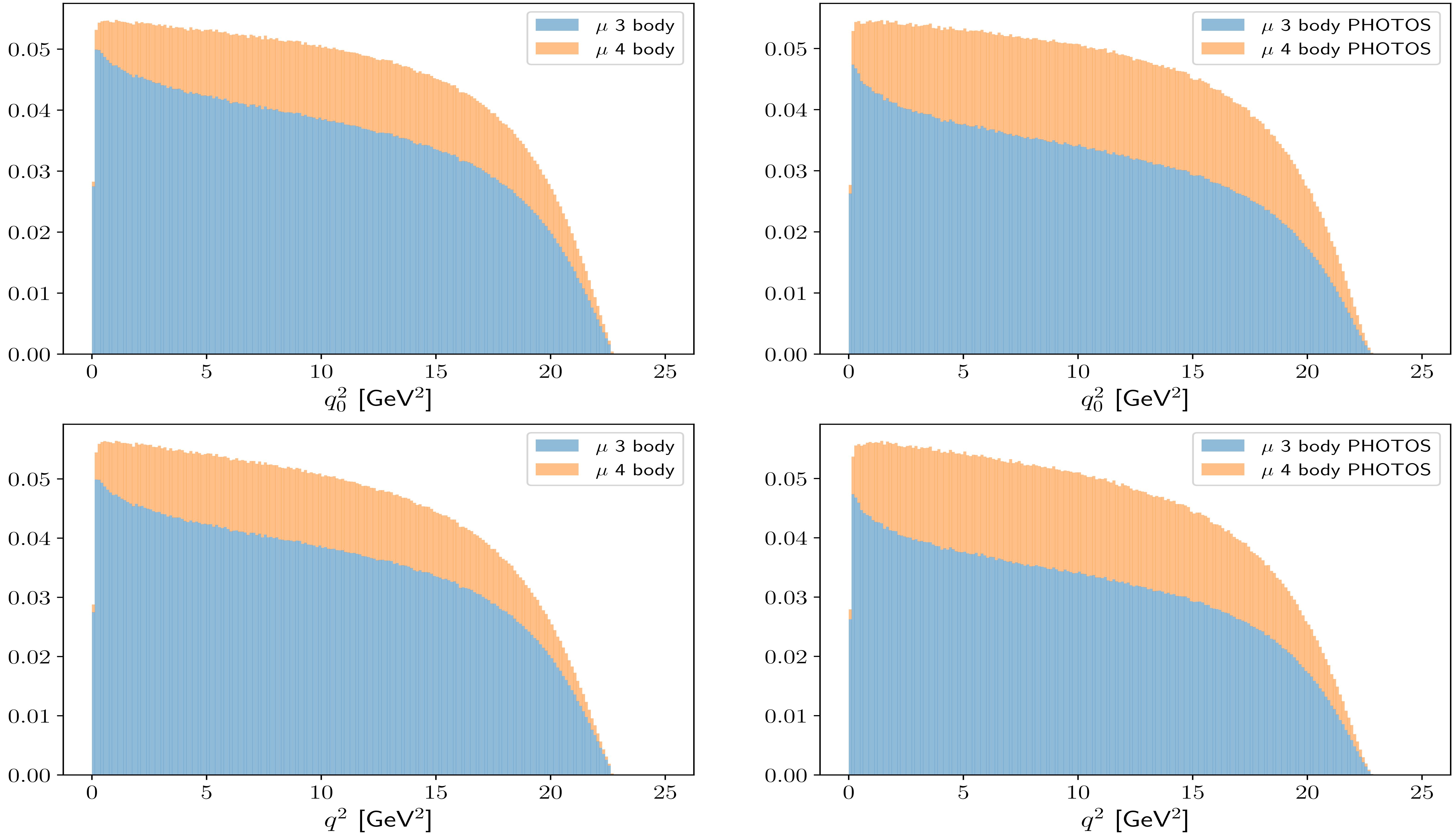

Our Monte Carlo results: q_0^2 spectrum comparison

- By taking the ratio of NLO/LO in our Monte Carlo generator we can derive the impact of QED corrections either on the q_0^2 spectra, for both μ/e

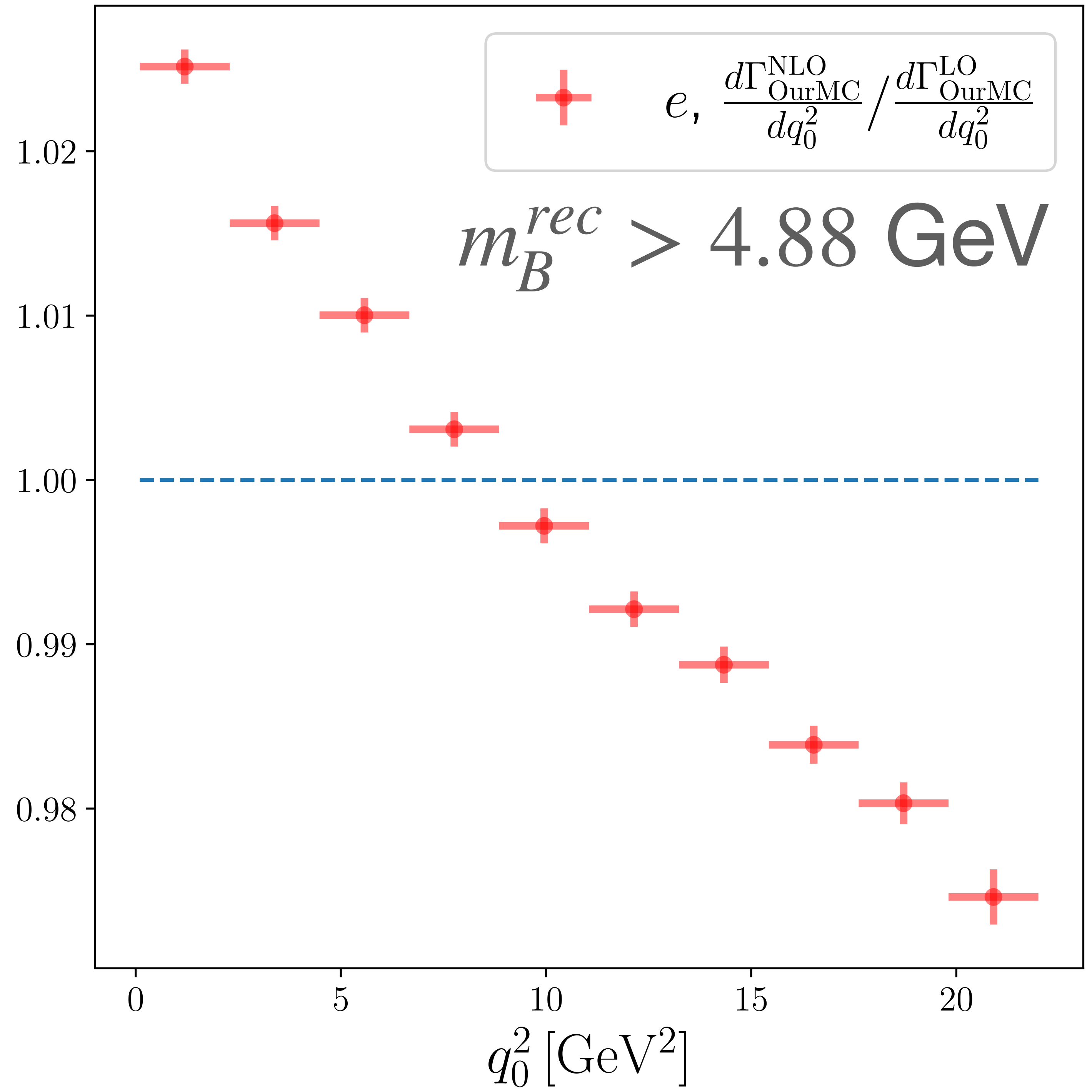

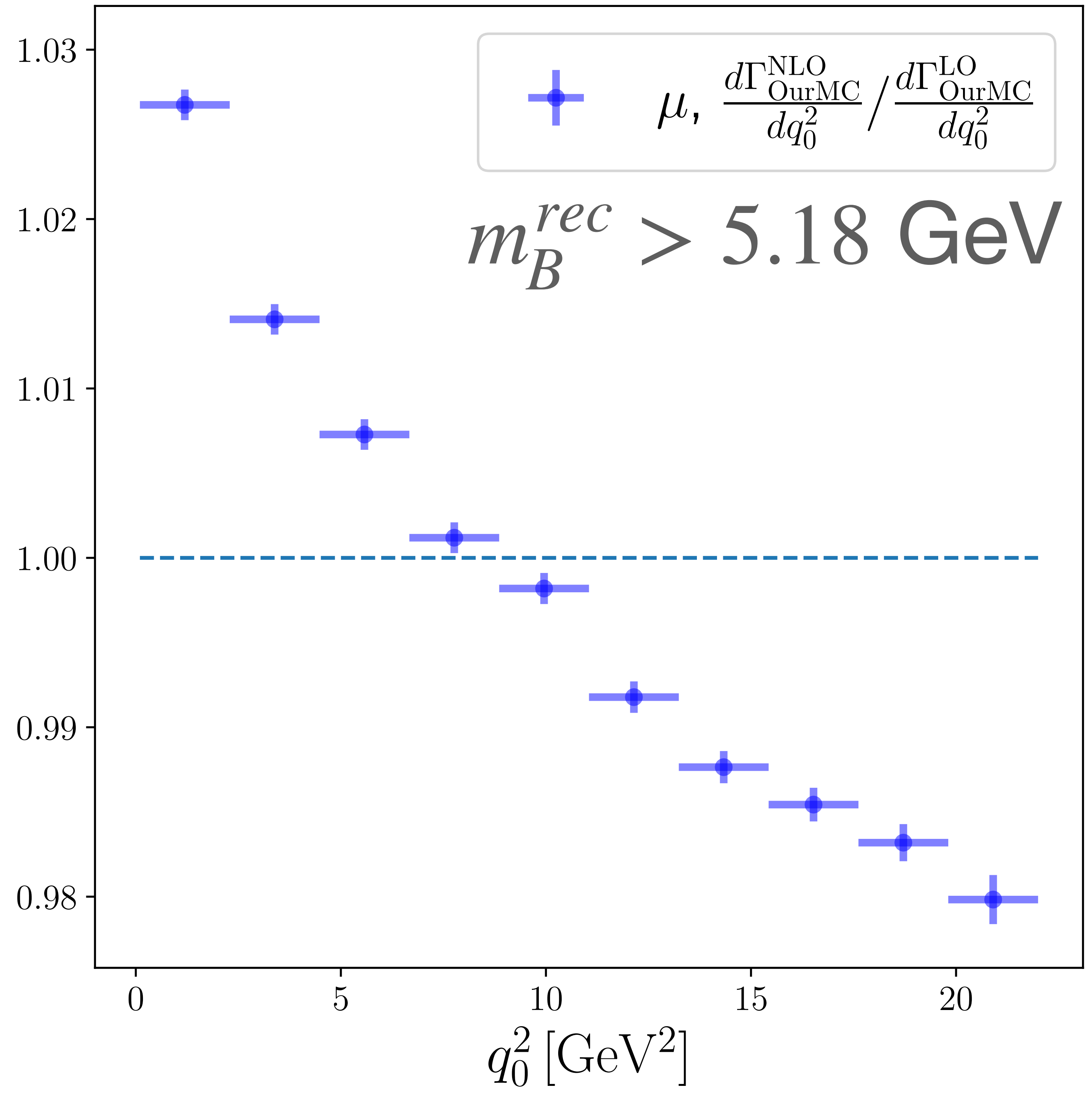

- Note: normalisation of these plots is arbitrarily obtained by normalising separately the NLO and LO distributions to unity

Our Monte Carlo results: q_0^2 spectrum comparison

- A comparison with [PHOTOS] is established by taking the ratio of the impact of QED corrections on the q_0^2 spectra, for both μ/e, between [PHOTOS] and our Monte Carlo approach

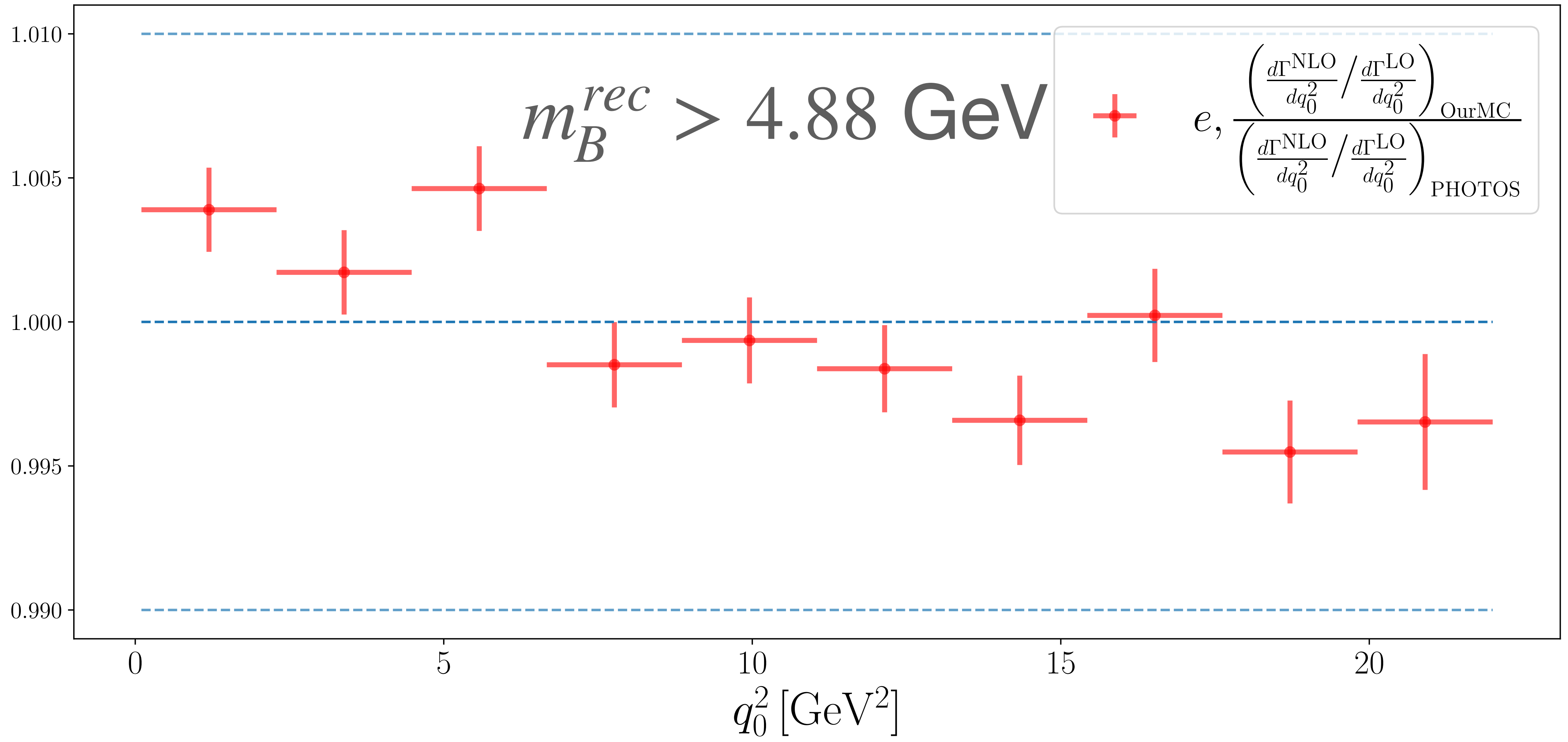

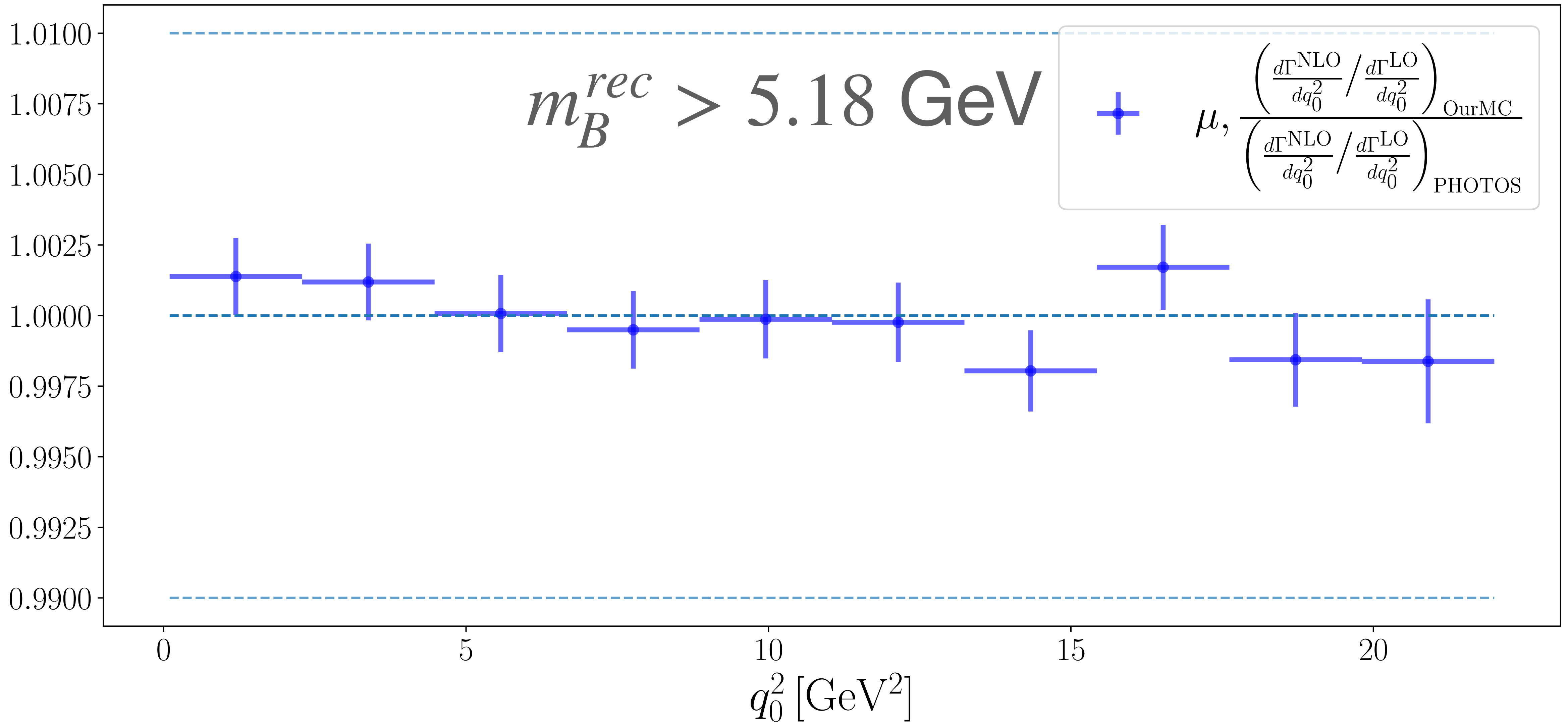

- Sub percent agreement between our Monte Carlo and PHOTOS is found in the q_0^2 variable

Our Monte Carlo results: q^2 spectrum comparison

- By taking the ratio of NLO/LO in our Monte Carlo generator we can derive the impact of QED corrections either on the q^2 spectra, for both μ/e

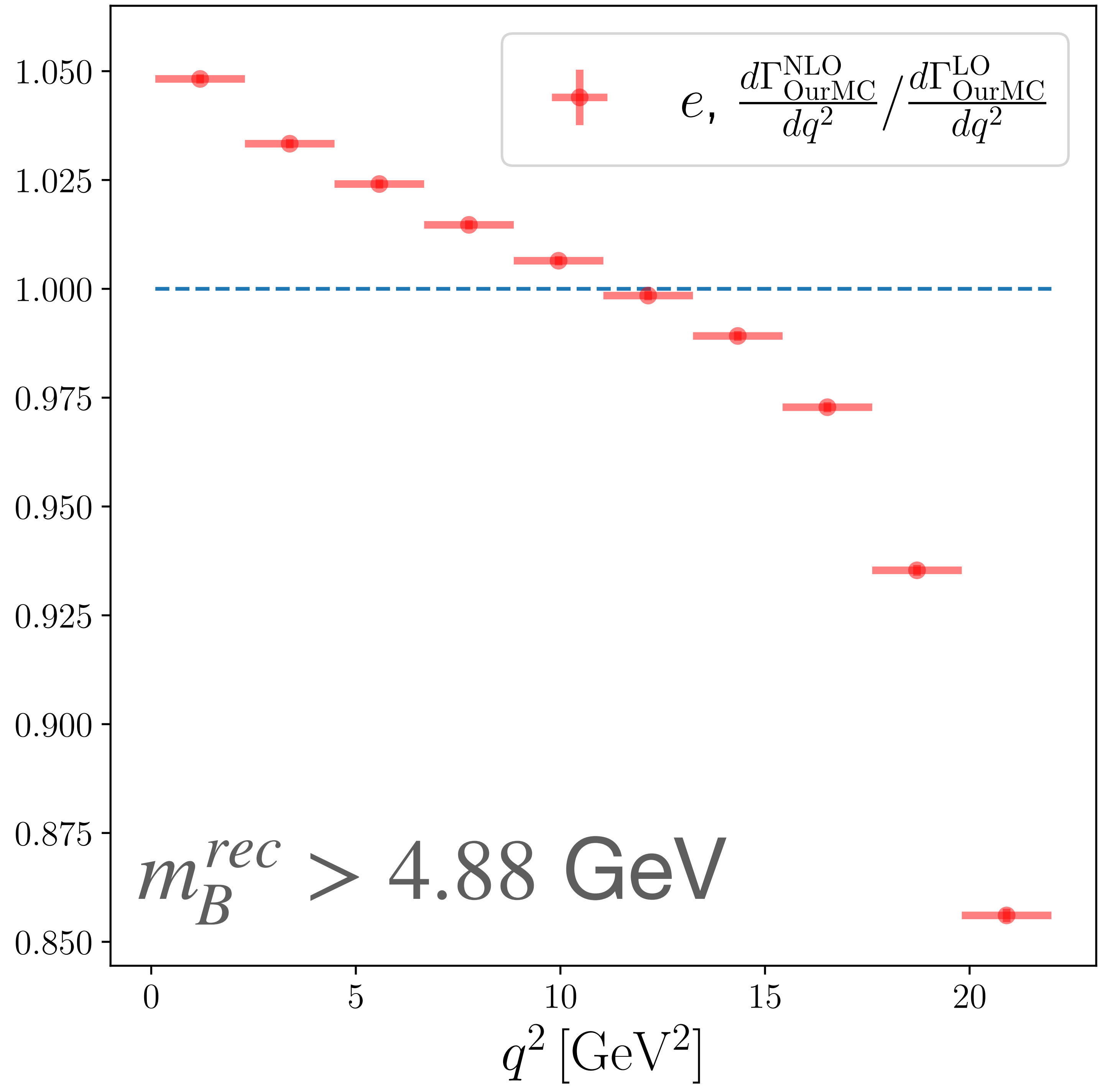

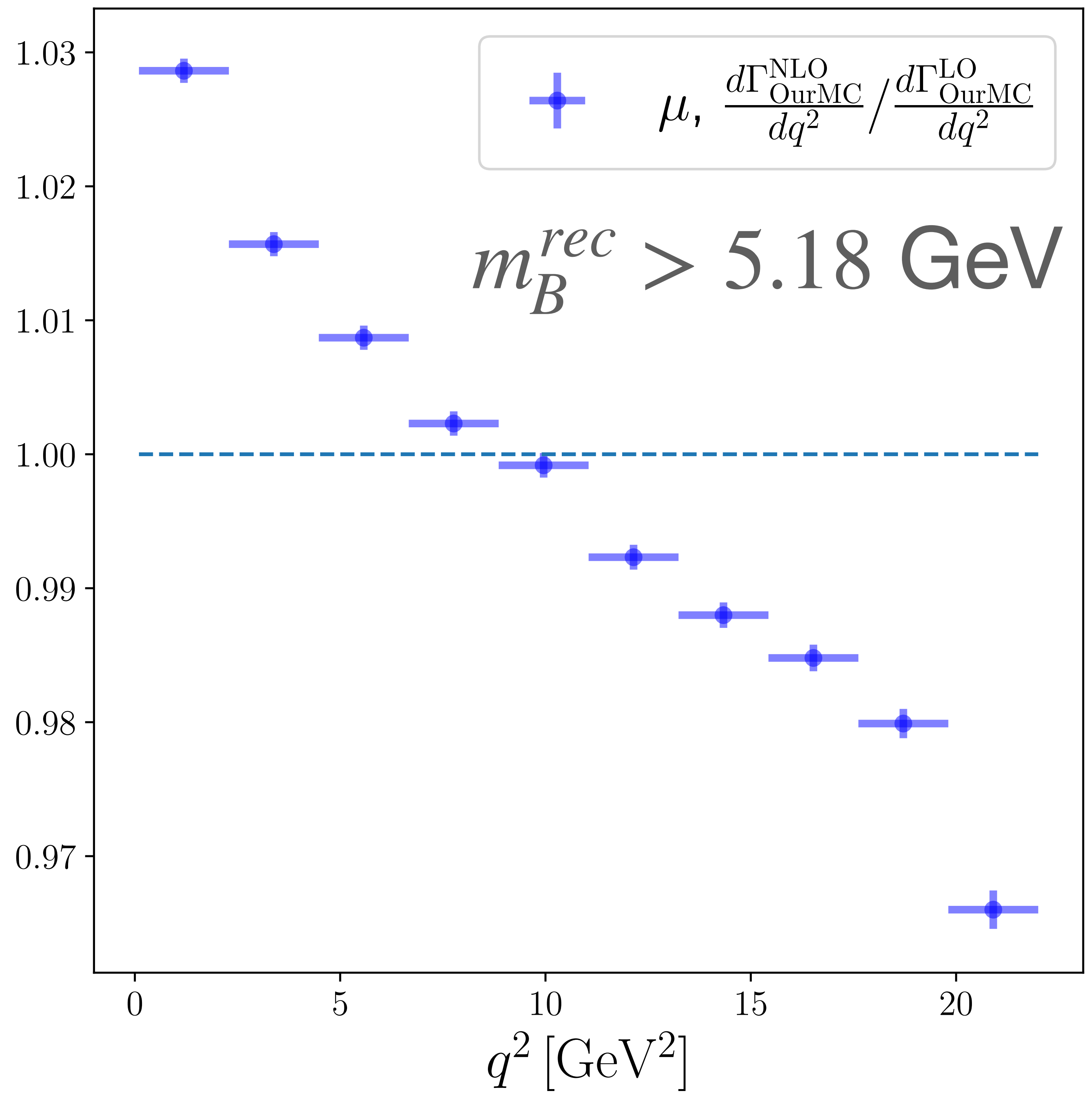

- <u>Note:</u> normalisation of these plots is arbitrarily obtained by normalising separately the NLO and LO distributions to unity

Our Monte Carlo results: q^2 spectrum comparison

- A comparison with [PHOTOS] is established by taking the ratio of the impact of QED corrections on the q^2 spectra, for both μ/e, between [PHOTOS] and our Monte Carlo approach

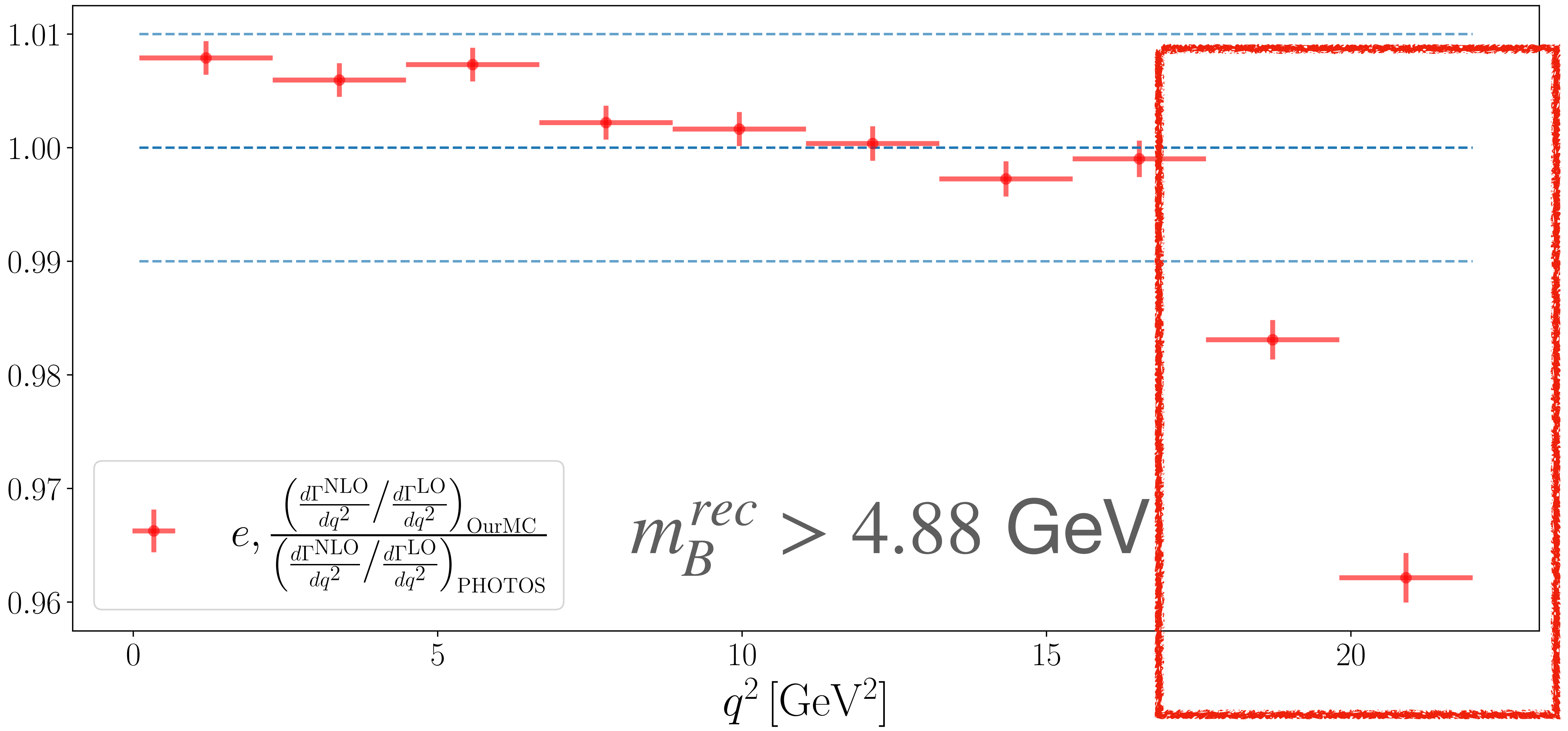

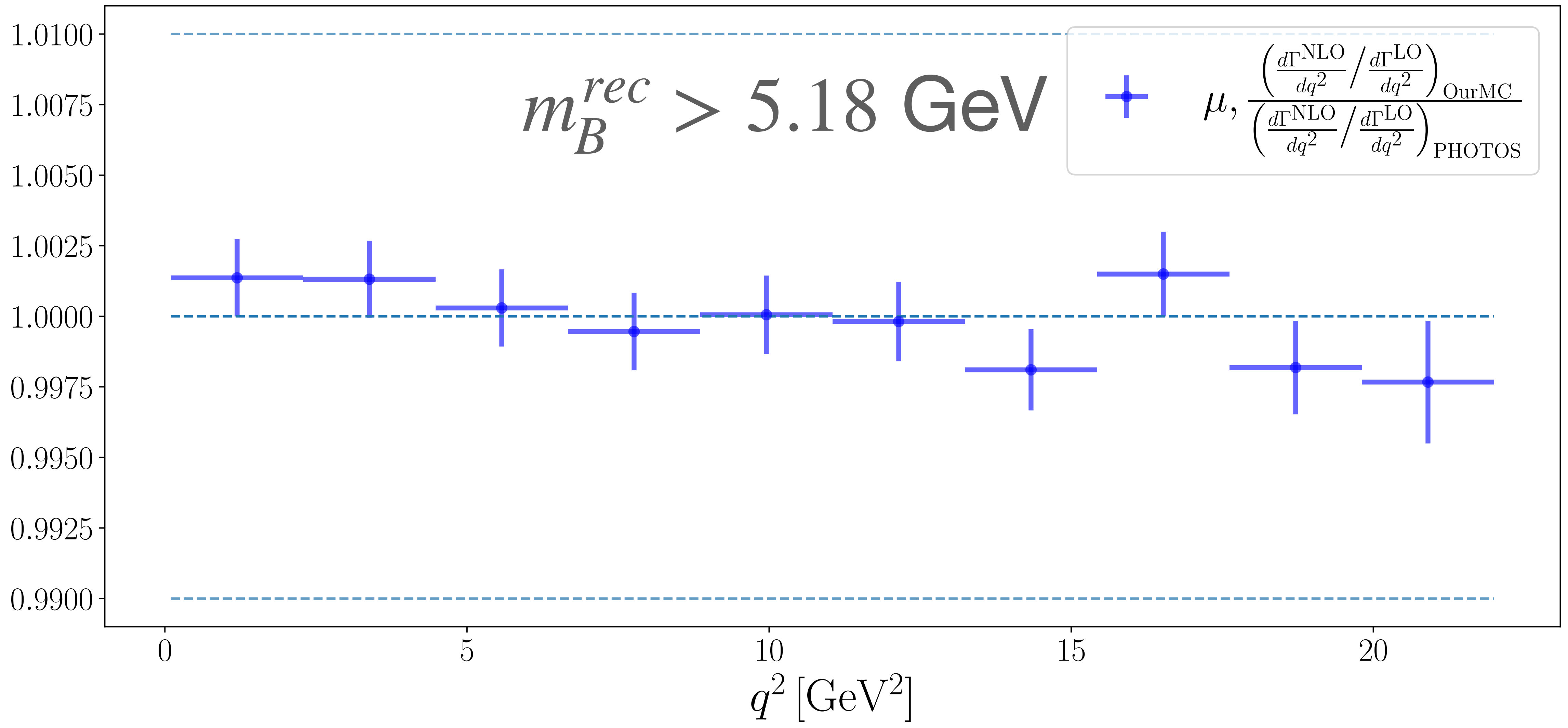

- O(4%) disagreement is found for e at high q^2 $\rightarrow$ originates from large corrections that go beyond the fixed $\mathcal{O}(\alpha)$ accuracy of our MC.

- At the kinematic endpoint, due to lack of available phase space for real radiation, corrections are of O(20%) and maximally imbalanced btw virtual and real emission.

Our Monte Carlo results: c_ℓ spectrum comparison

- By taking the ratio of NLO/LO in our Monte Carlo generator we can derive the impact of QED corrections either on the c_ℓ spectra, for both μ/e

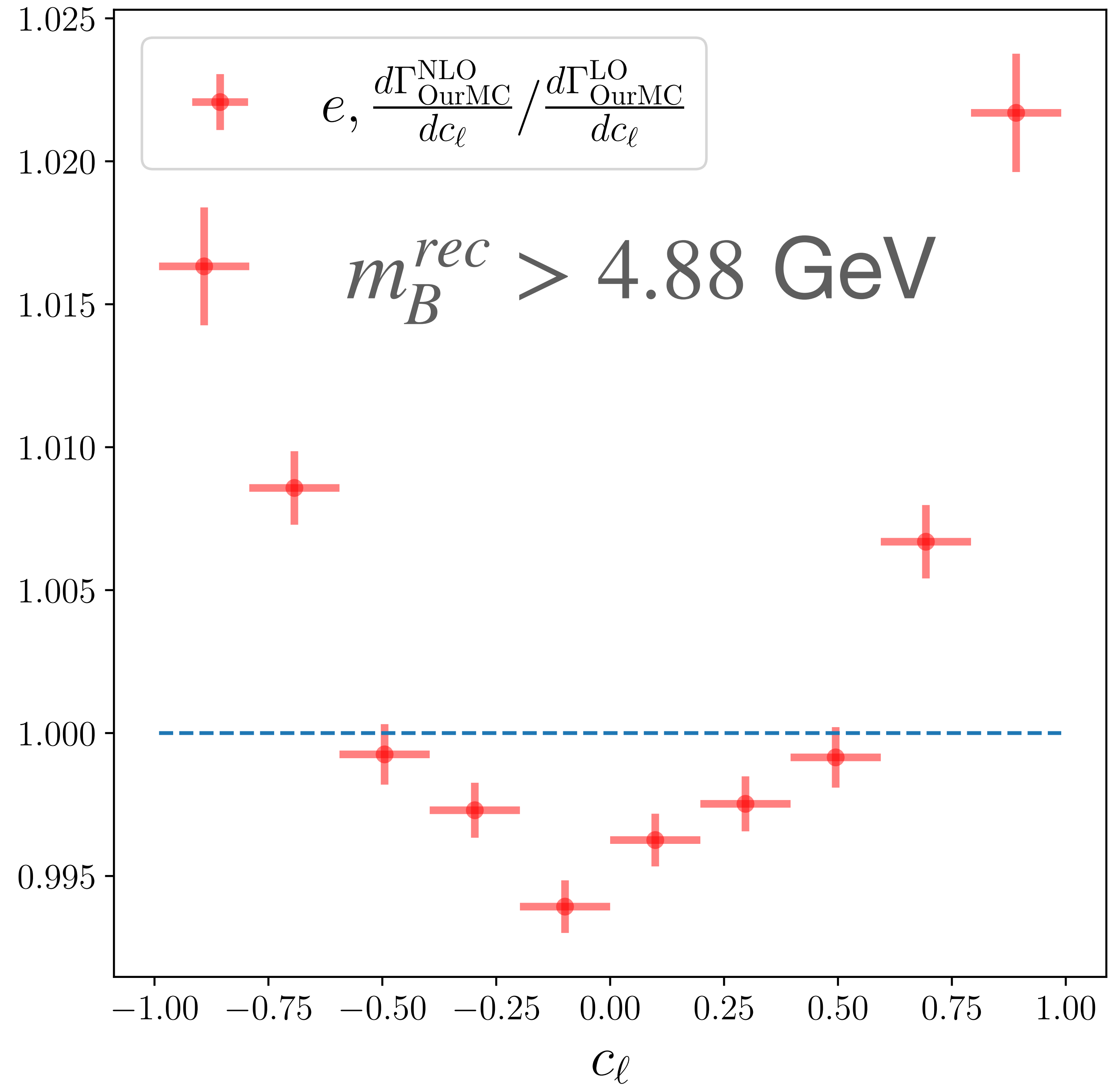

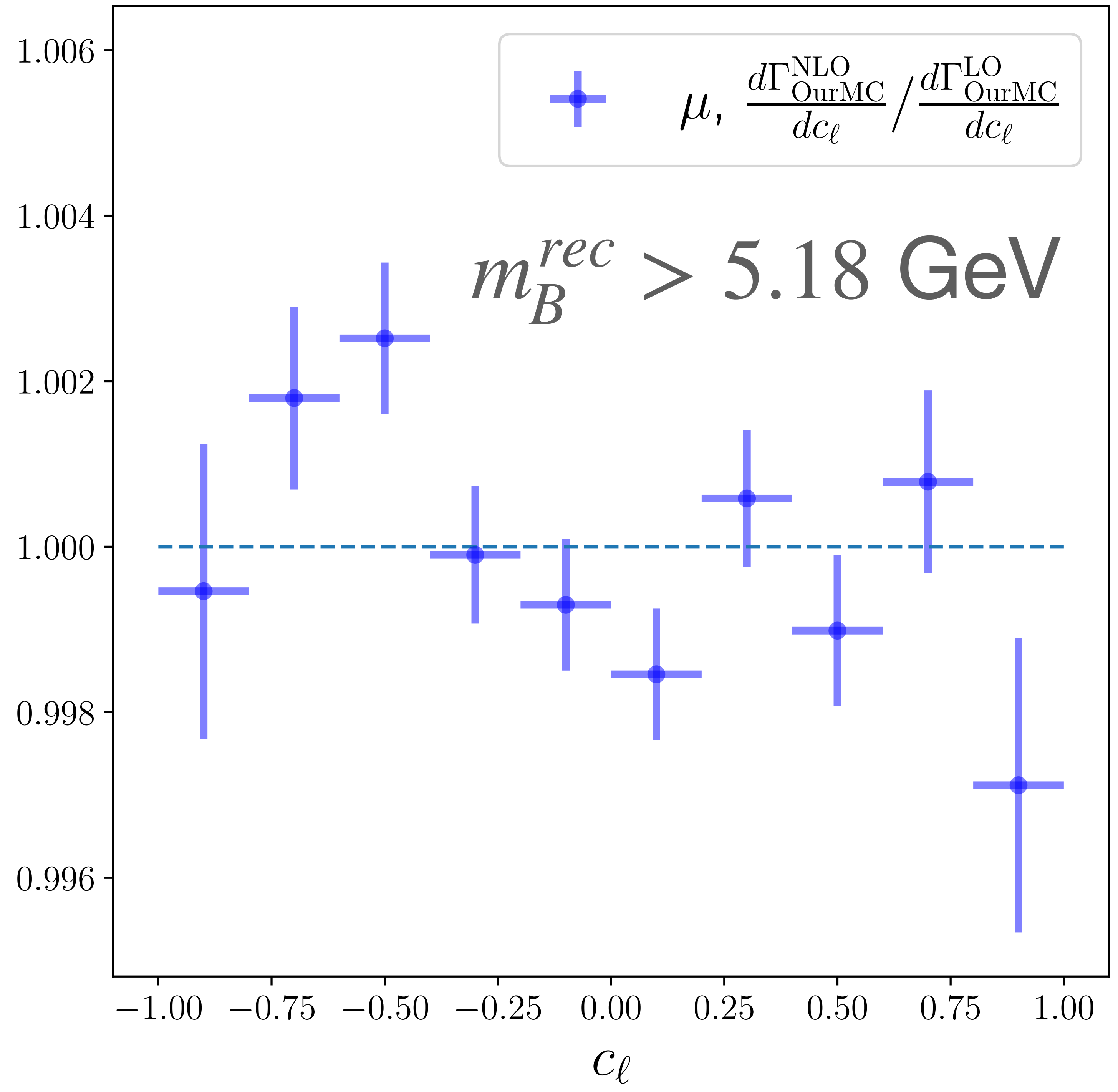

- Note: normalisation of these plots is arbitrarily obtained by normalising separately the NLO and LO distributions to unity

Our Monte Carlo results: c_ℓ spectrum comparison

- A comparison with [PHOTOS] is established by taking the ratio of the impact of QED corrections on the c_ℓ spectra, for both μ/e, between [PHOTOS] and our Monte Carlo approach

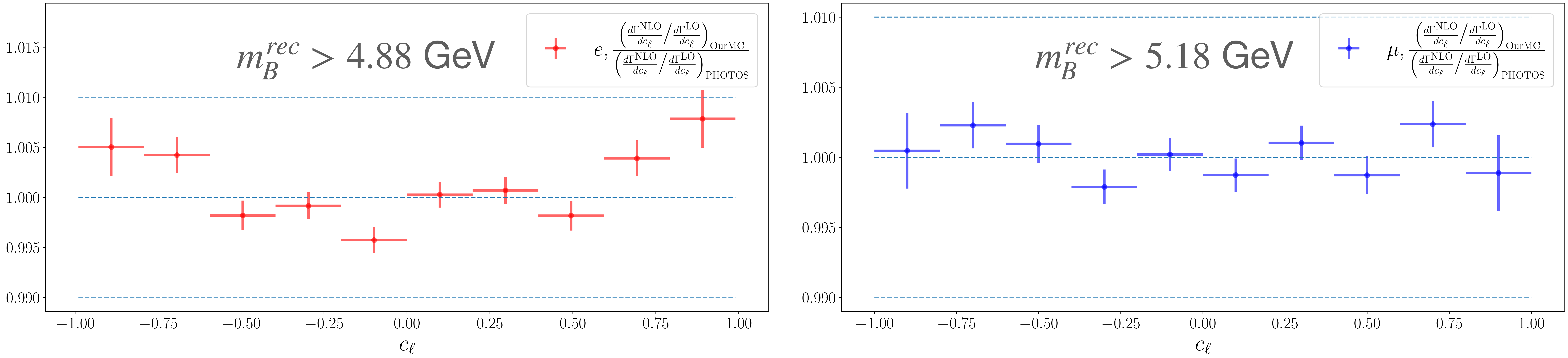

- Sub percent agreement between our Monte Carlo and PHOTOS is found in the c_ℓ variable

Including the J/ψ resonance

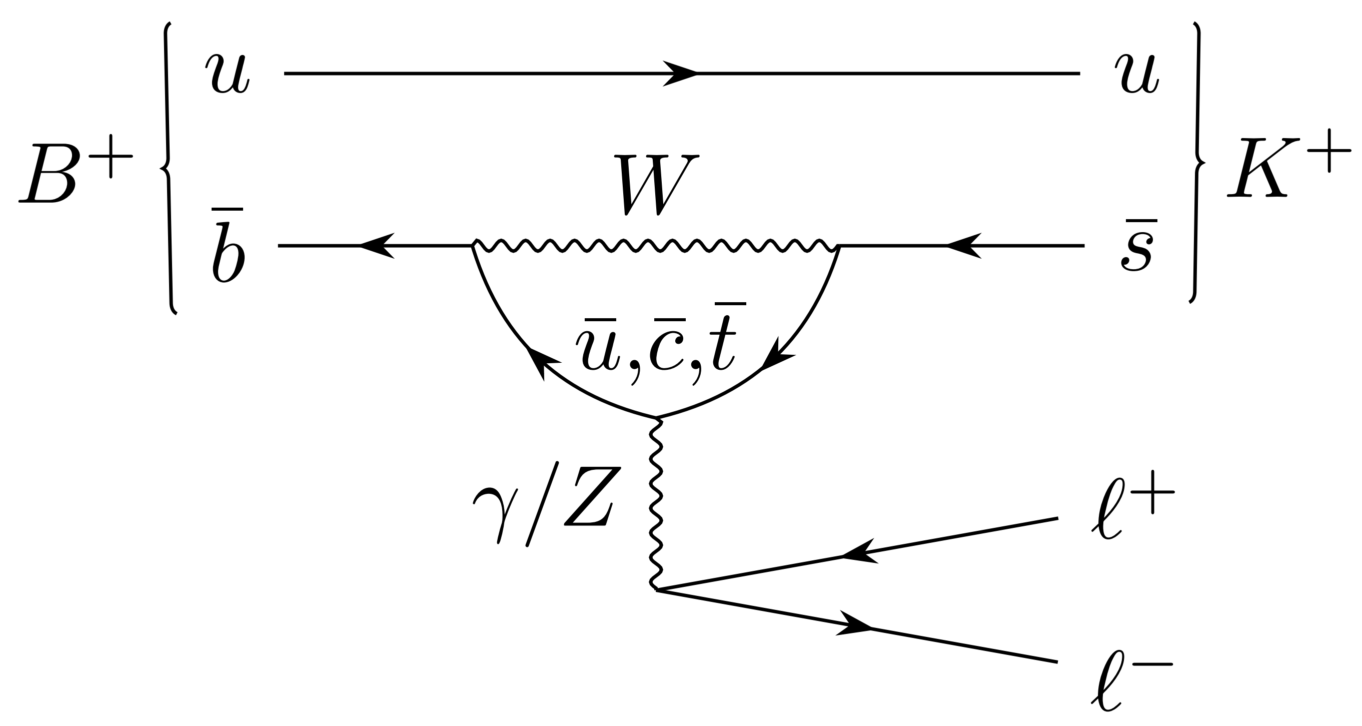

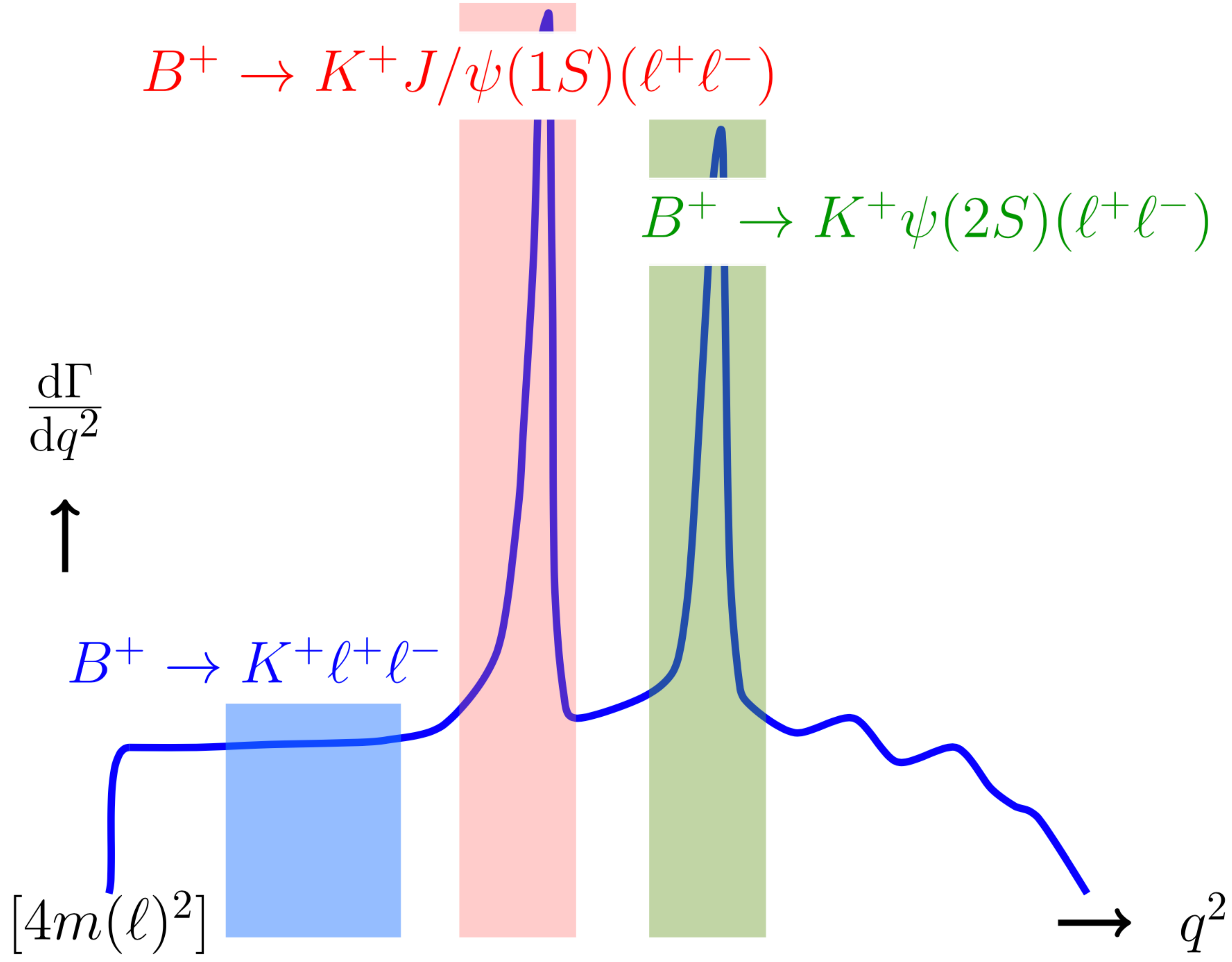

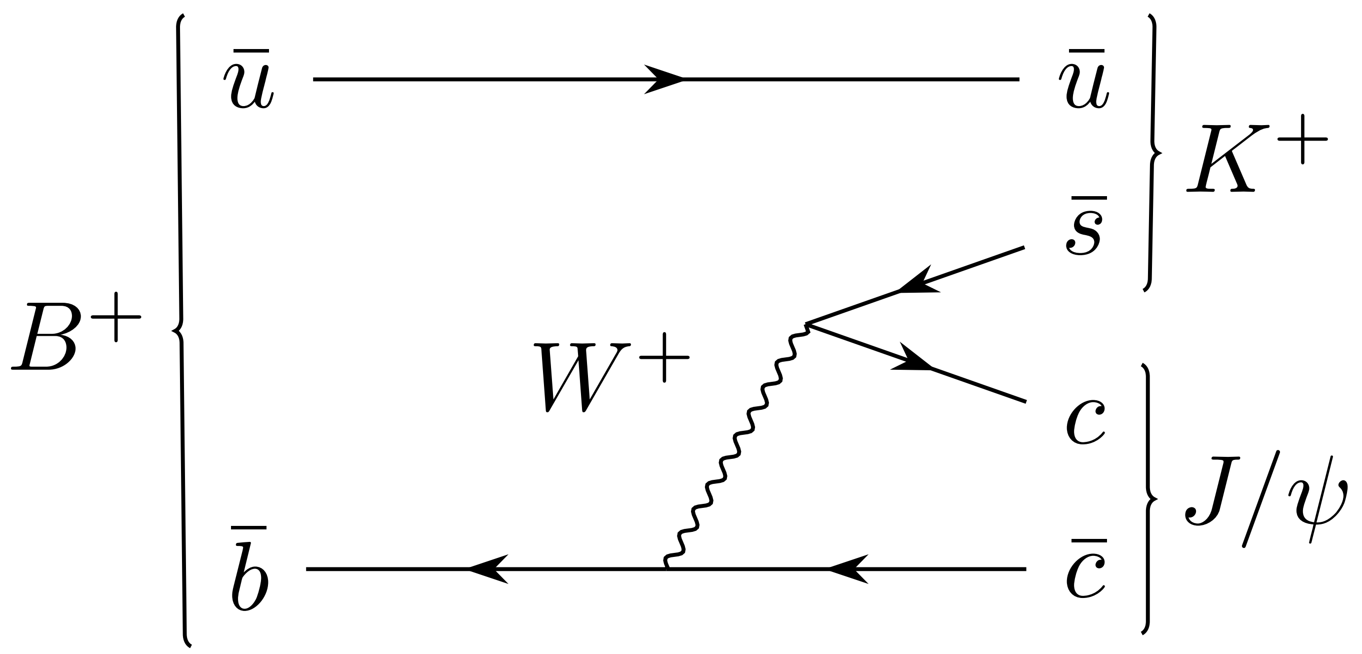

- Regions at $q^2 \sim m^2_{J/\psi}, m^2_{\psi(2S)}$ dominated by resonances $\rightarrow$ used as control channels
- Rare mode extends throughout the q^2 range, but is selected in a region away from charmonium resonances
- However in analysis rare and resonant modes are simulated separately, could this induce a non universal effect between μ/e

Including the J/ψ resonance: method

- In order to include QED effects induced by the J/ψ resonance we perform a modification of C_9:

$$C_9 \to C_9^{eff} = C_9 + \Delta C_9(q^2)$$

See Saad's Talk

- This however introduces some technical difficulties in the event generation:
  - The modulus squared of the resonant amplitude $\mathscr{A}(B \to J/\psi(\ell^+\ell^-)K)$ is not included in generation due to excessively low sampling efficiencies at the J/ψ peak
  - Events are generated up to a maximum q_0^2 threshold such that the decay width is still positive and can be interpreted as a PDF, the maximum q_0^2 is chosen so that the bulk of the interference effect is captured
  - Due to low sampling efficiency a fake lepton of mass $10 \cdot m_e$ is simulated

Including the J/ψ resonance: results

- We simulated the two extreme cases in which $\delta_{J/\psi} = 0, \pi/2$ although we know from [1612.06764] that the worst case scenario of maximal interference is not favoured by the data

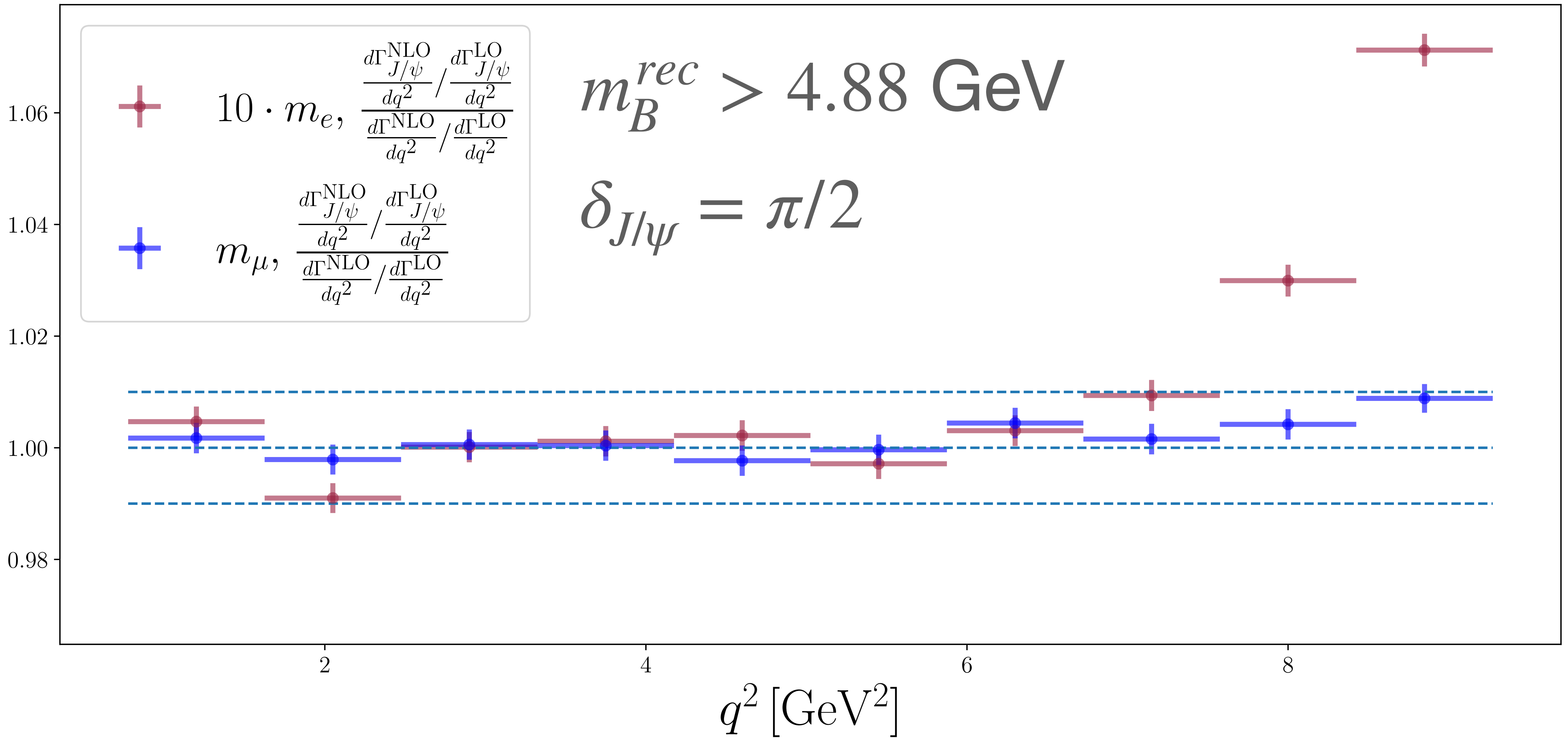

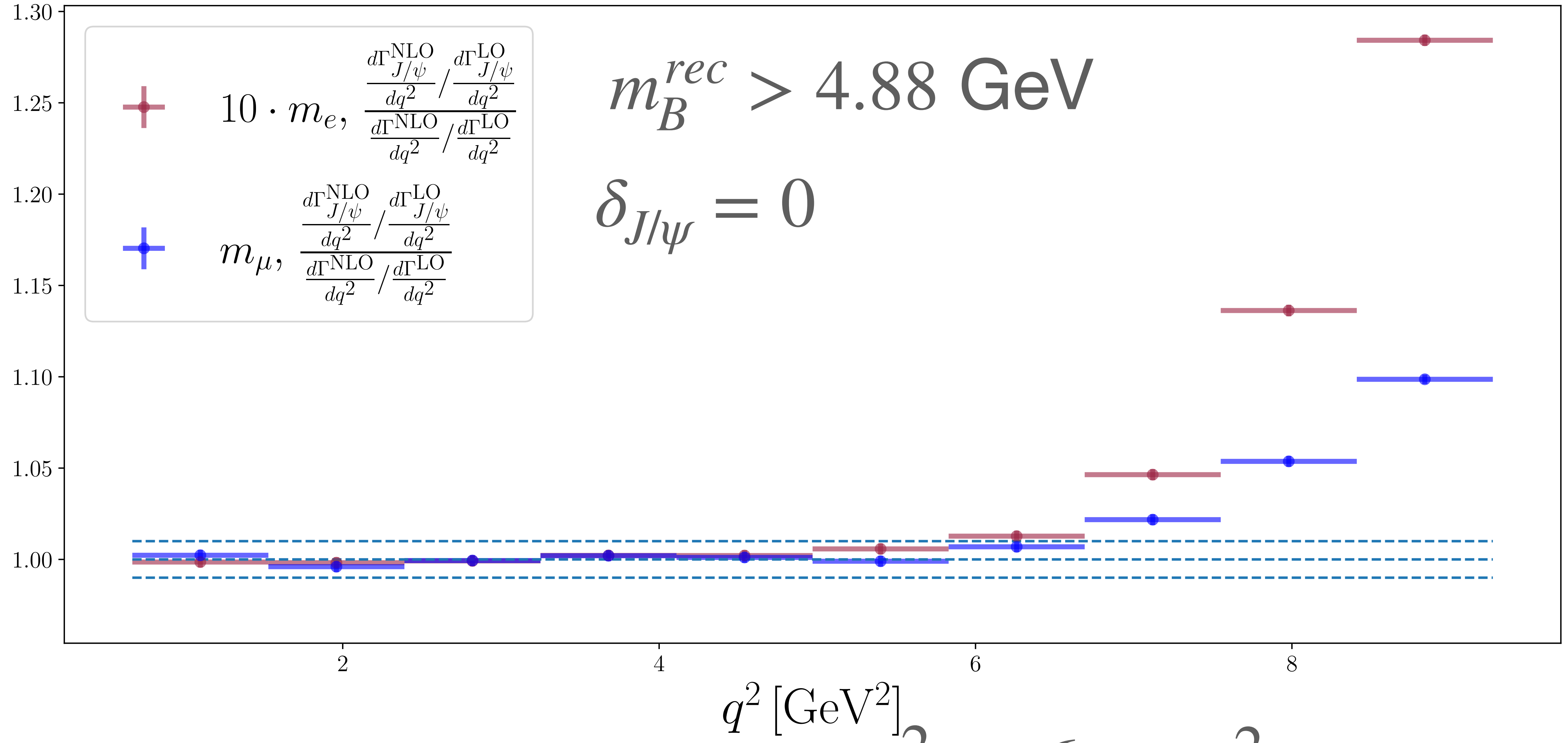

- The effects of the J/ψ interference term are below the percent level for $q^2 < 6$ GeV^2

Bremsstrahlung recovery at LHCb

- The upstream $e^{\pm}$ track is extrapolated to the ECAL
- All $E_T > 75$ reconstructed neutral clusters, compatible with the $e^{\pm}$ trajectory, are added back to the electron momentum
- Shortcomings
  - Poor energy resolution of ECAL
  - Brem can be out of acceptance
- Electrons with brem recovered have
  - Better momentum resolution
  - Better PID ($\pi^{\pm}$ don't emit brem)

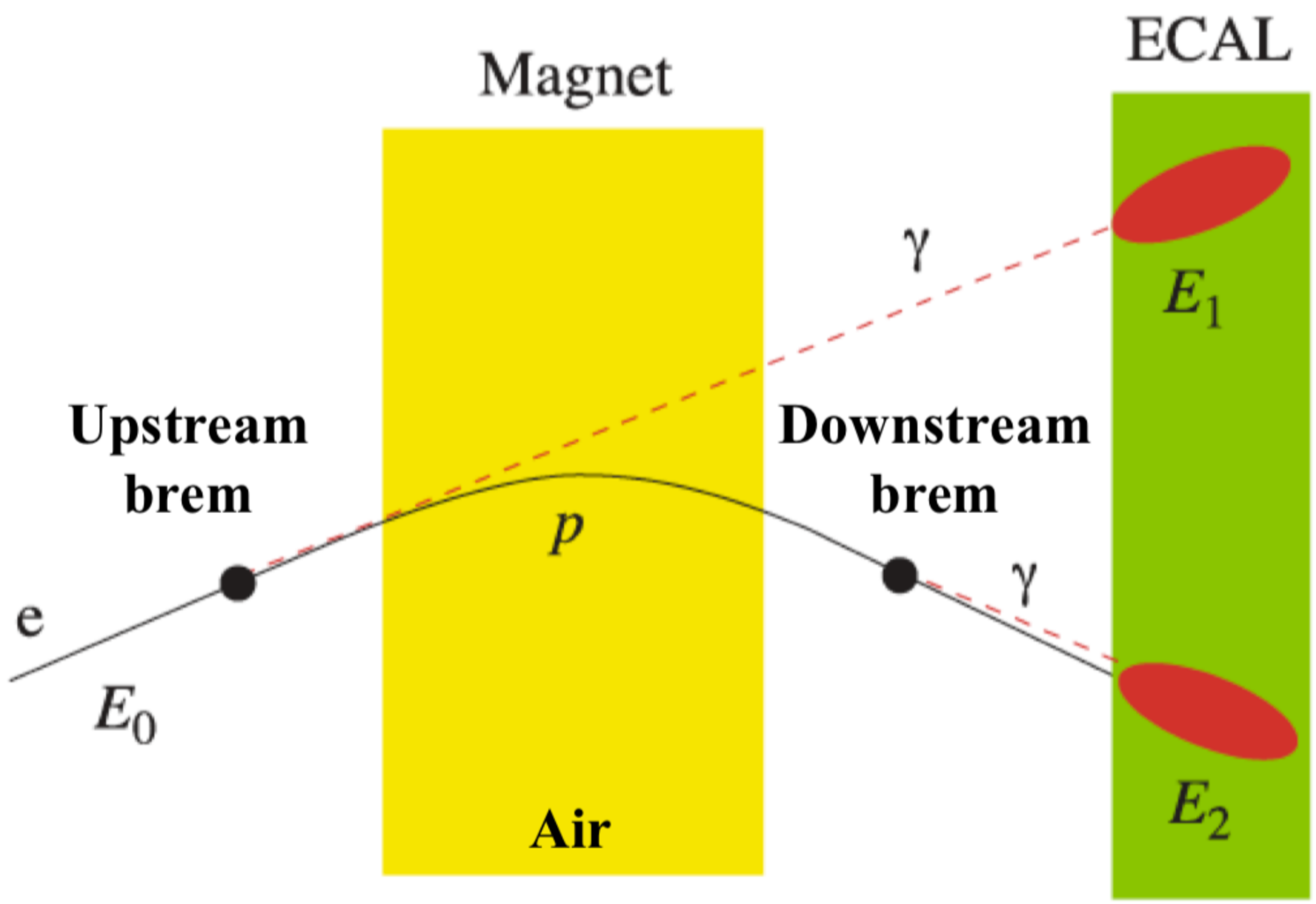

Bremsstrahlung recovery at LHCb

- In the hypothesis of:
  - An $e^{\pm}$ emits at most one bremsstrahlung photons
  - And the probability of brem recovery is uncorrelated between e^{+} and e^{-}

$$
\begin{aligned}
1 &= f^{ee}_{2\mathrm{cl}} + f^{ee}_{1\mathrm{cl}} + f^{ee}_{0\mathrm{cl}} \\
&= P^2 + 2P(1-P) + (1-P)^2 \\
&\Rightarrow P \simeq 50\,\%
\end{aligned}
$$

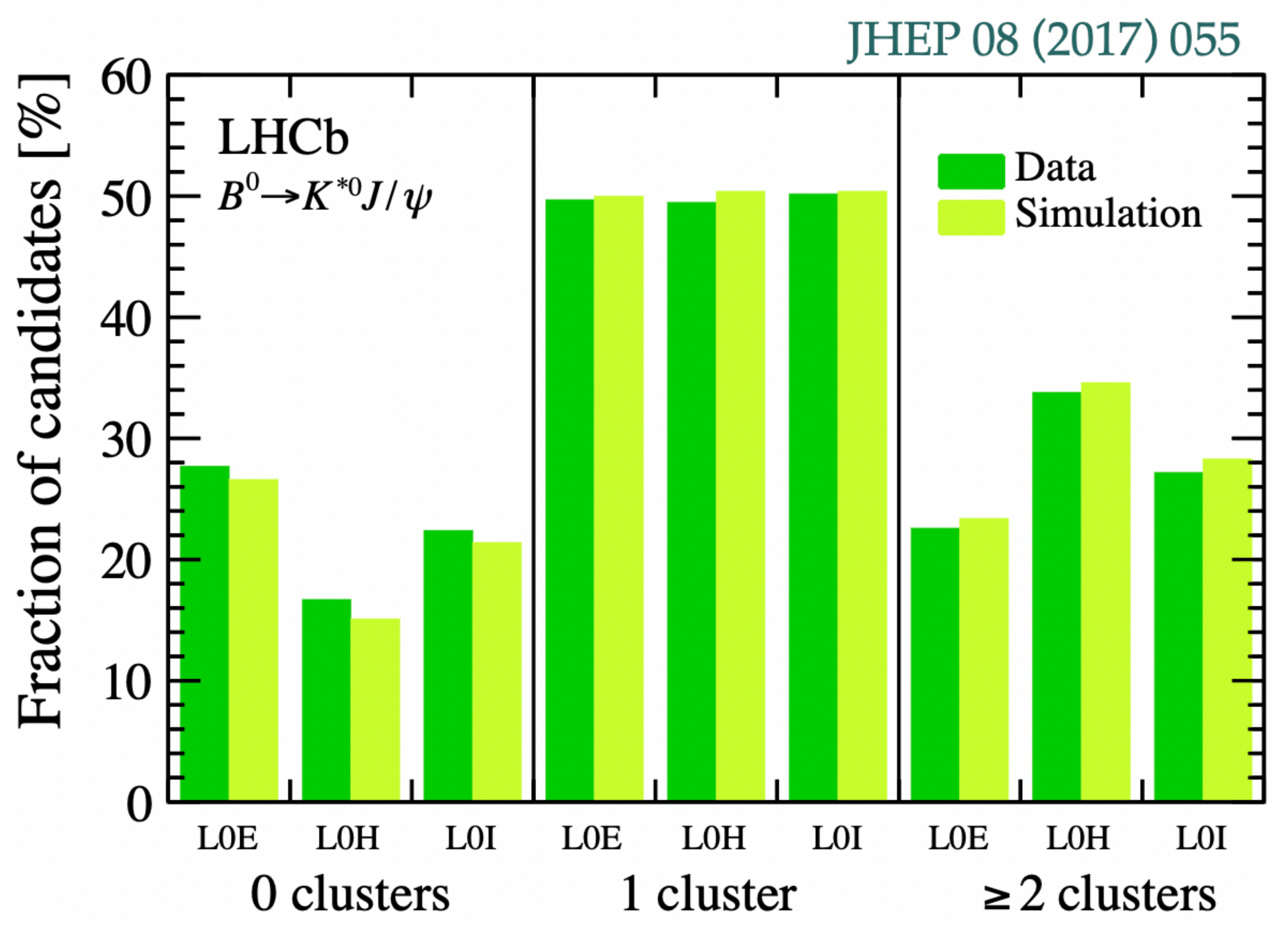

Effects of brem recovery on the mass resolution

[NPHYS-2021-03-00814B]

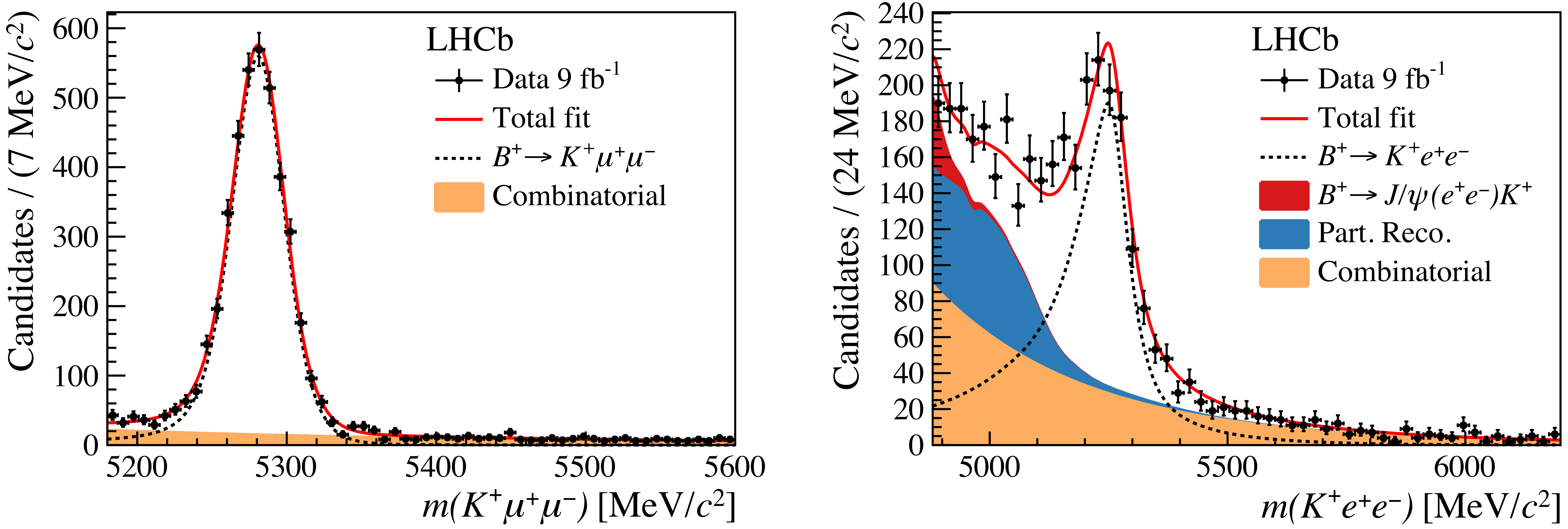

Conclusions

- We have built a NLO Monte Carlo event generator for the $\bar{B} \to \bar{K}\ell^+\ell^-$ that includes all infrared sensitive logs, at the full differential level
- We have shown with a custom Monte Carlo approach that [PHOTOS] correctly describes the distortions of the q^2 , q_0^2 distributions, as well as the c_ℓ, due to QED corrections.
- By including the interference term of the rare mode with the resonant J/ψ mode in our simulation, we have shown that neglecting it's modelling in current experiments is a good approximation

Backup

$B^+ \to K^+\ell^+\ell^-$

[PRL 122 (2019) 191801]

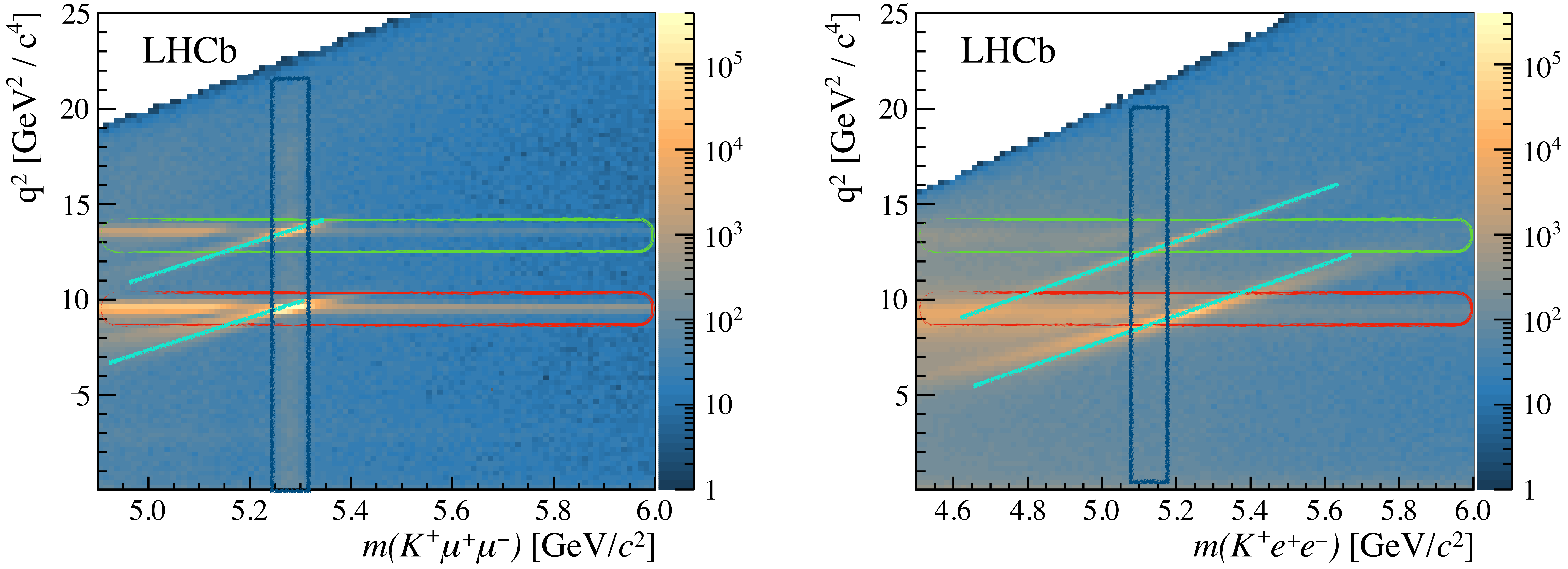

- Peaking structures: $B^+ \to K^+J/\psi(\ell^+\ell^-)$ and $B^+ \to K^+\psi(2S)(\ell^+\ell^-)$ (resonant decay modes)
- Diagonal elongations: radiative tails + incorrectly-added bremsstrahlung
- Vertical band: $B^+ \to K^+\ell^+\ell^-$ (rare decay mode)

R_K measurement at LHCb

Control electron-muon differences using double ratio between nonresonant $B^+ \to K^+\ell^+\ell^-$ and resonant $B^+ \to K^+J/\psi(\ell^+\ell^-)$.

$$R_K = \frac{N(K^+\mu\mu)}{N(K^+J/\psi(\mu\mu))}\boxed{\frac{\varepsilon(K^+J/\psi(\mu\mu))}{\varepsilon(K^+\mu\mu)}} \Bigg/ \frac{N(K^+ee)}{N(K^+J/\psi(ee))}\boxed{\frac{\varepsilon(K^+J/\psi(ee))}{\varepsilon(K^+ee)}}$$

- High statistics of the resonant mode;
- Similar kinematics of rare and resonant mode leads to suppression of systematic uncertainties;
  - Identical selection up to $m(K^+\ell^+\ell^-)$ and q^2 for rare and resonant modes
- $r_{J/\psi}$ known to be LFU within 0.4% [PDG] $\to$ used as a cross check

Analysis outline

1. Resonant modes yields extracted from a fit to the selected data samples.

2. Efficiencies are calculated from simulation and corrected using control mode data samples.

3. Estimation of systematic uncertainties.

4. Cross-checks with LFU channels such as $r_{J/\psi}$ are conducted.

5. Fit to the rare mode data $\rightarrow R_K$ is extracted.

Selection

[arXiv:2103.11769]

Requirements on reconstructed data, unchanged w.r.t. previous R_K analysis

- High quality tracks and reconstructed B^+ decay vertex
- Particle identification (PID) on kaon and lepton candidates, to suppress background from mis-ID
- Trigger requirements (more on next slide)
- Mass vetoes in order to suppress semileptonic cascades
- Multivariate selection to suppress combinatorial background

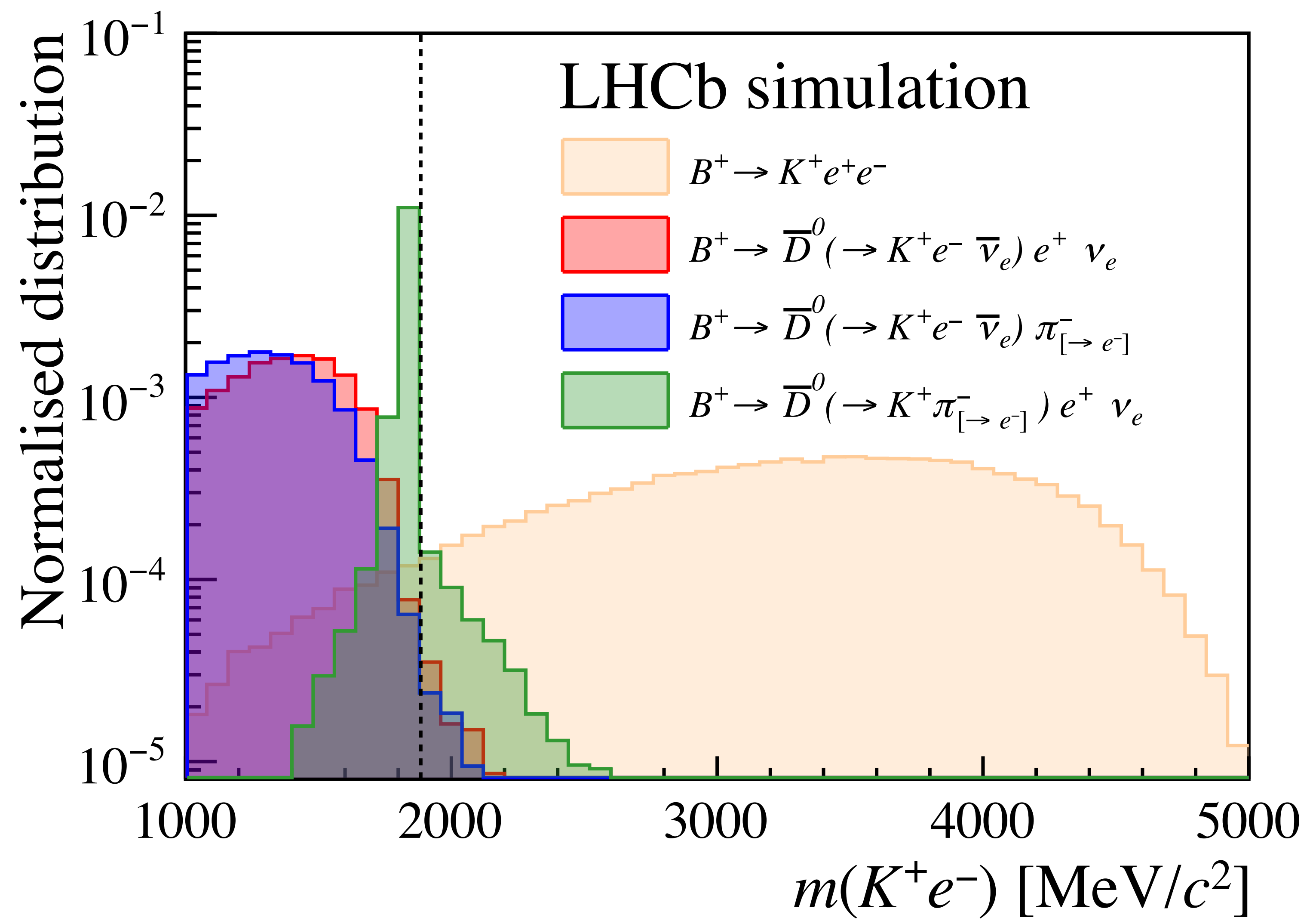

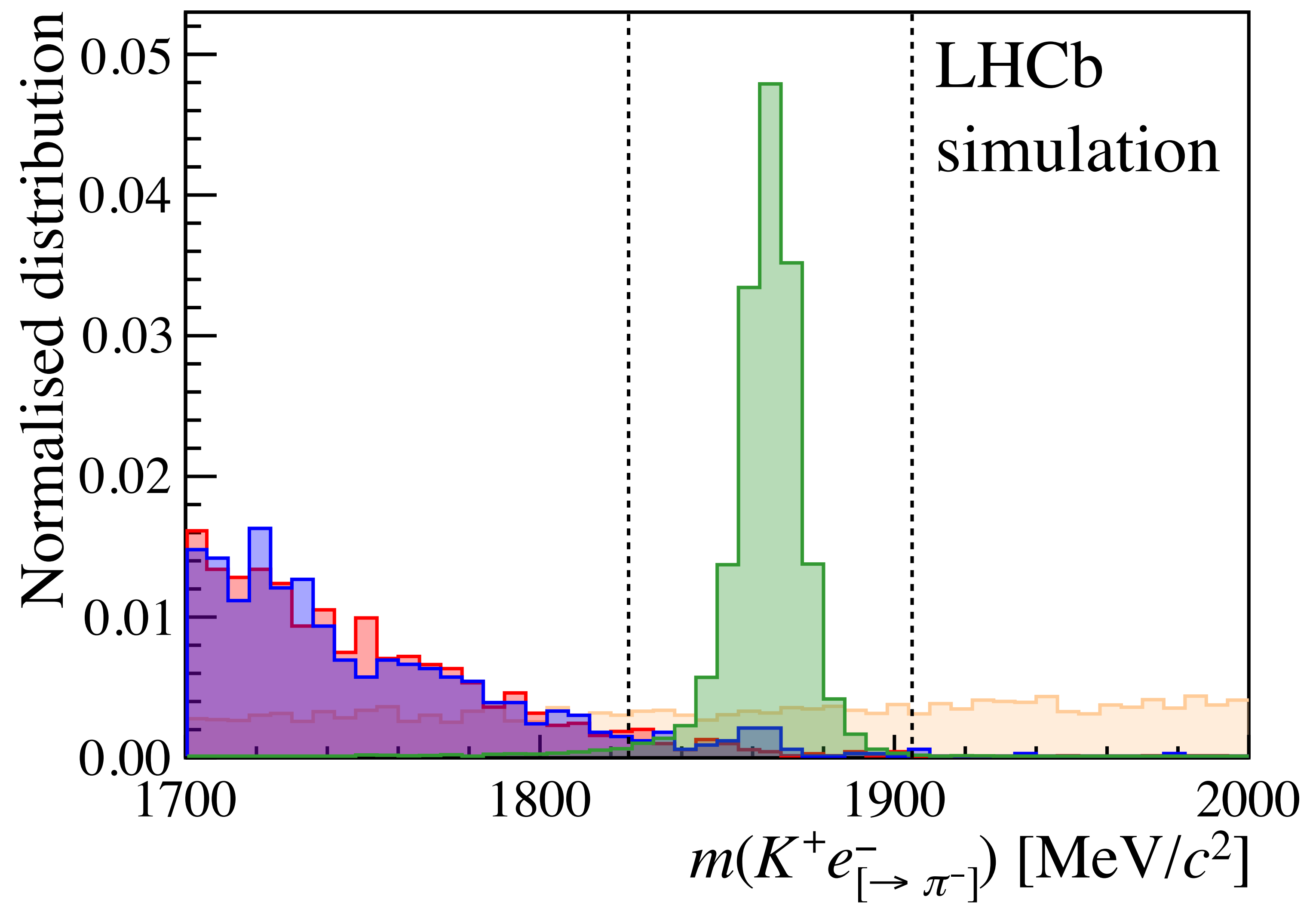

Trigger strategy

- For muon channels, trigger on L0 Muon
- For electron channels, three exclusive trigger categories:

  L0 Electron, L0 Hadron and L0 TIS.

- Systematics evaluated and cross-checks performed individually on each trigger category

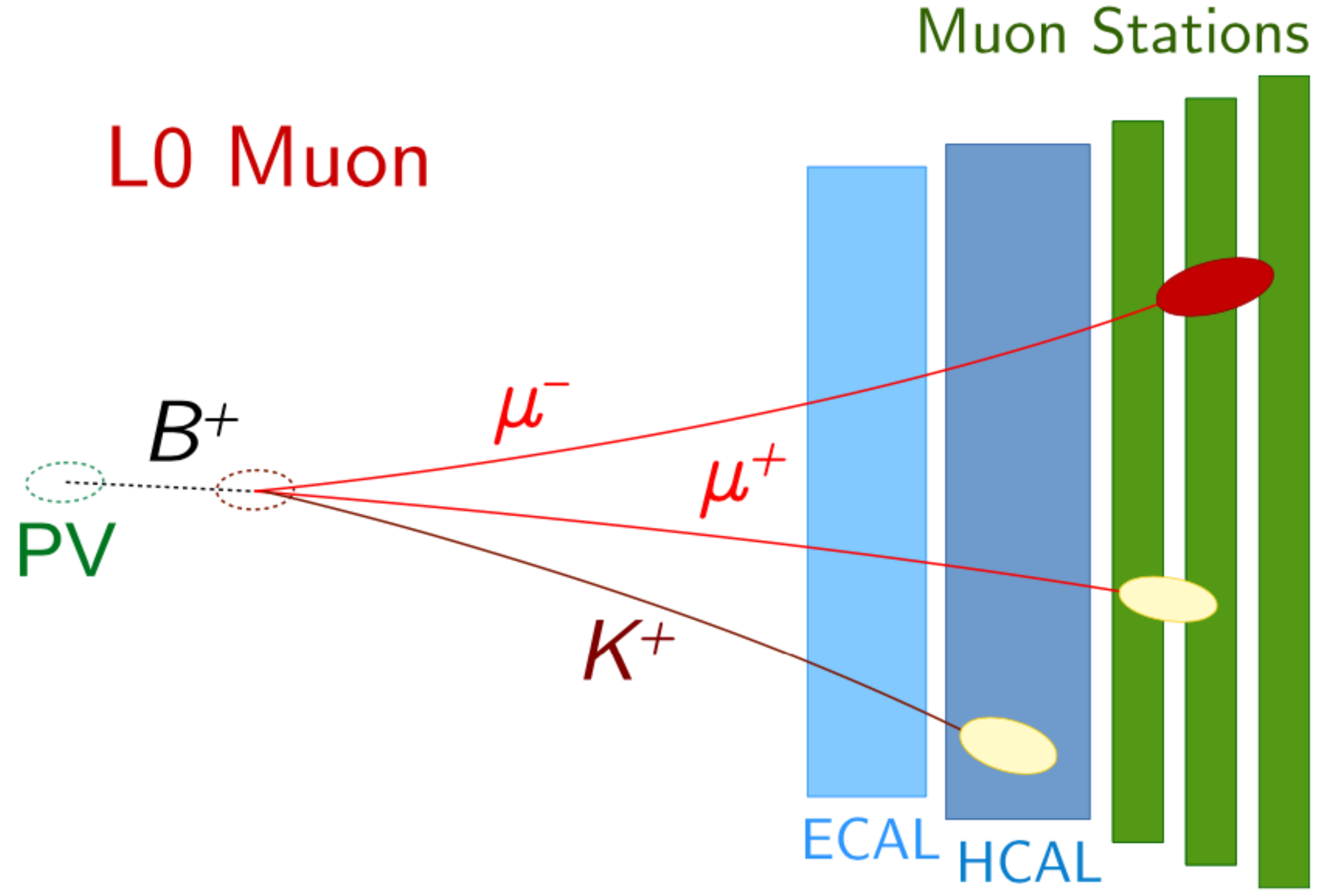

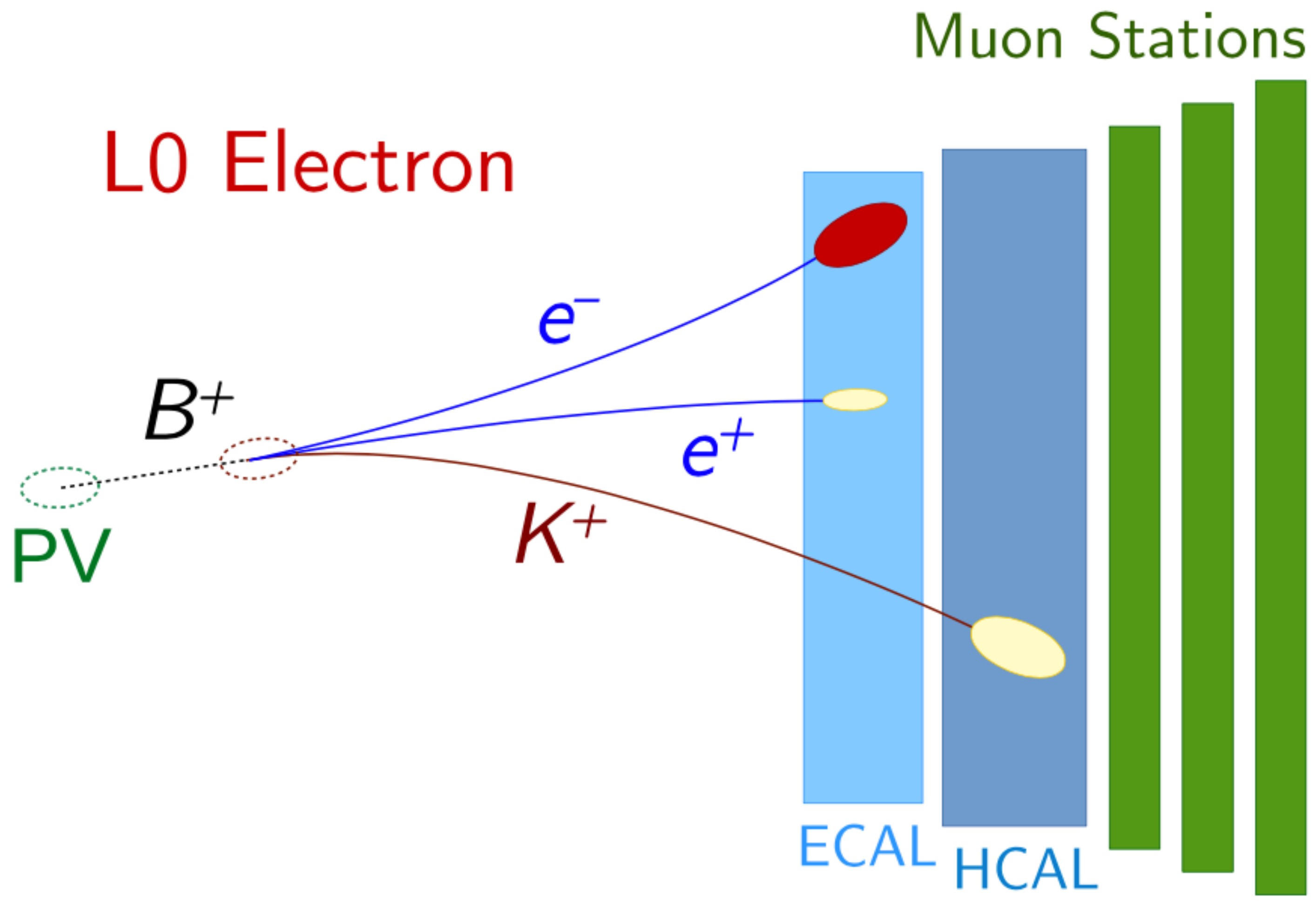

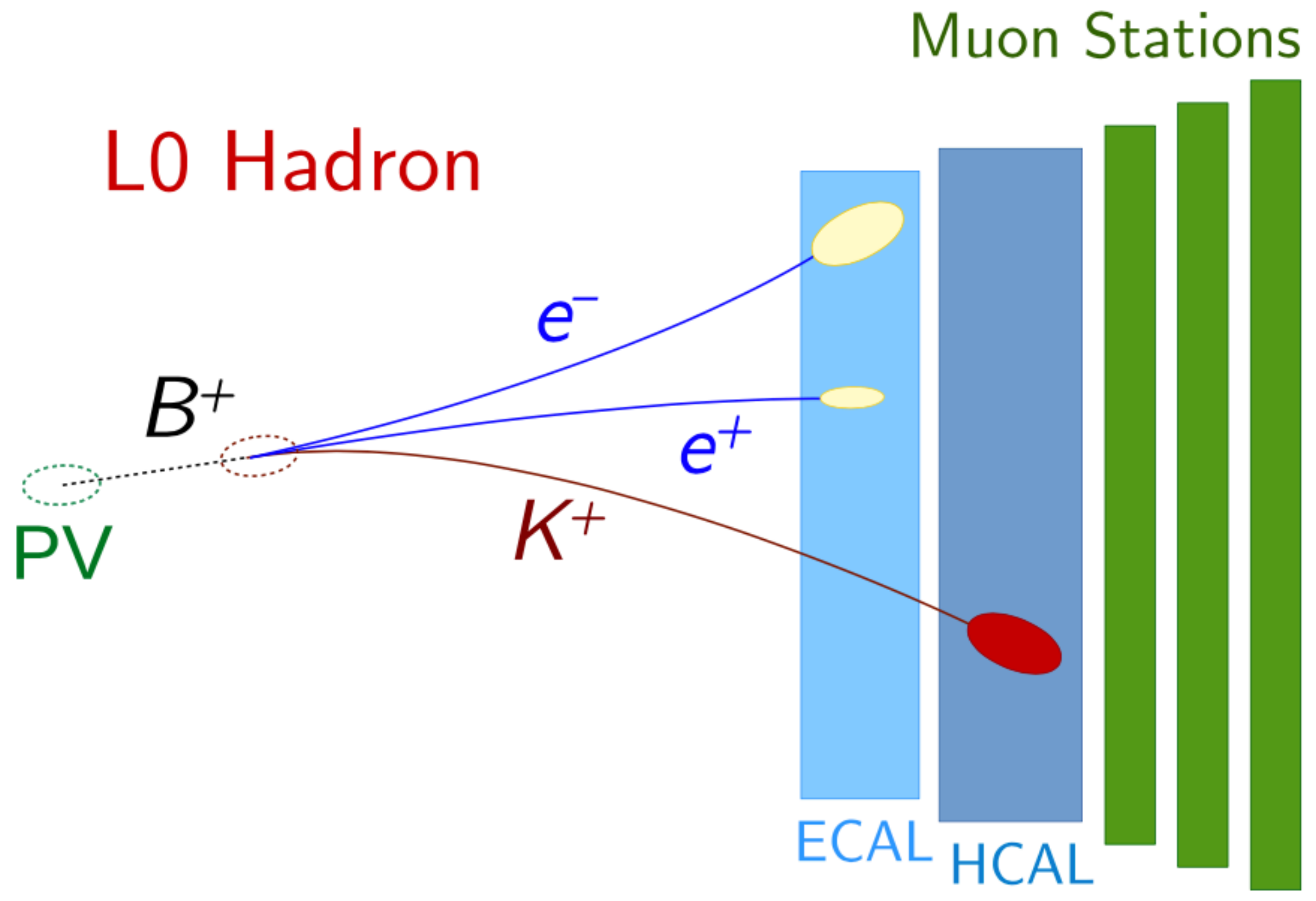

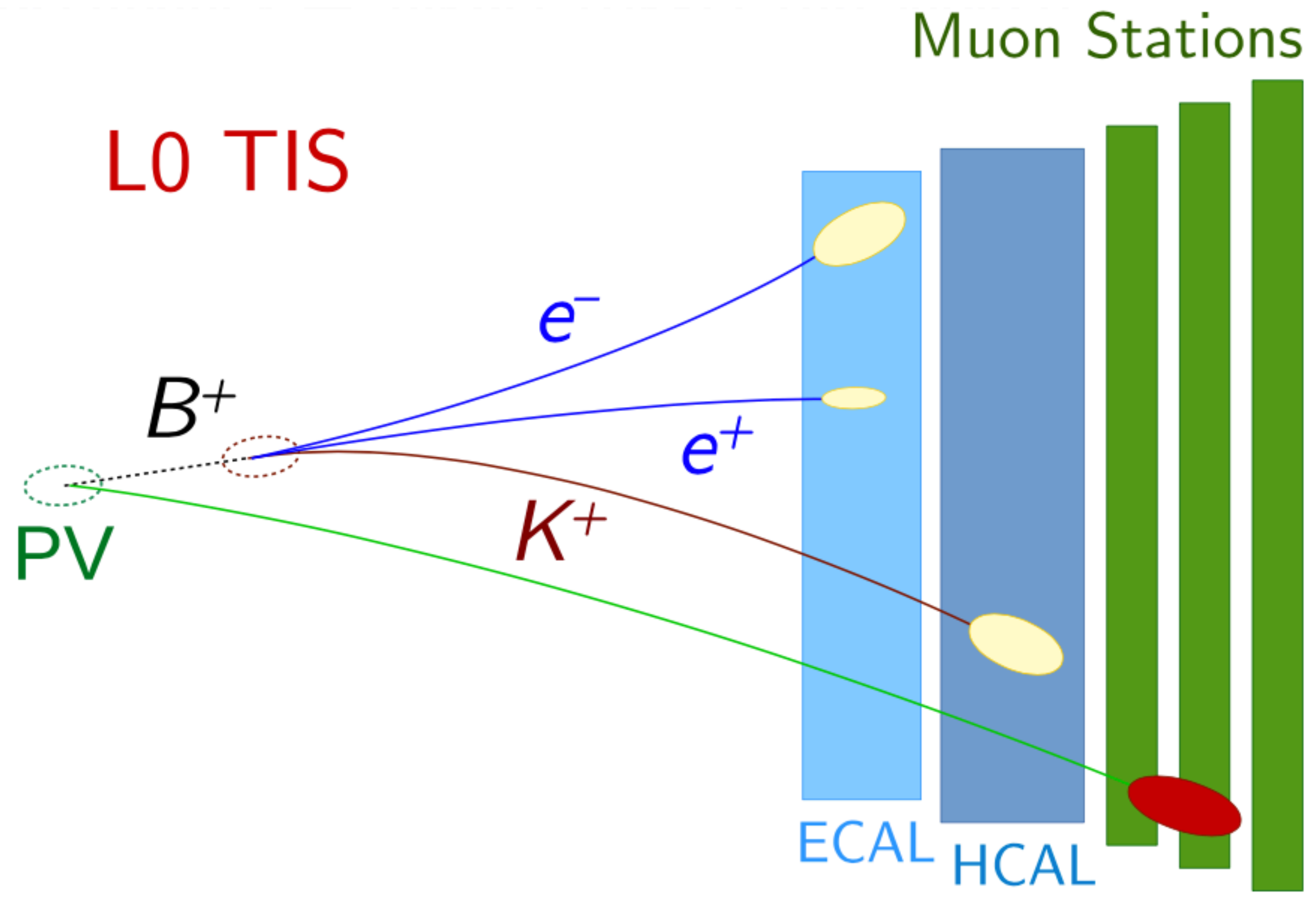

Fits to the control modes

[arXiv:2103.11769]

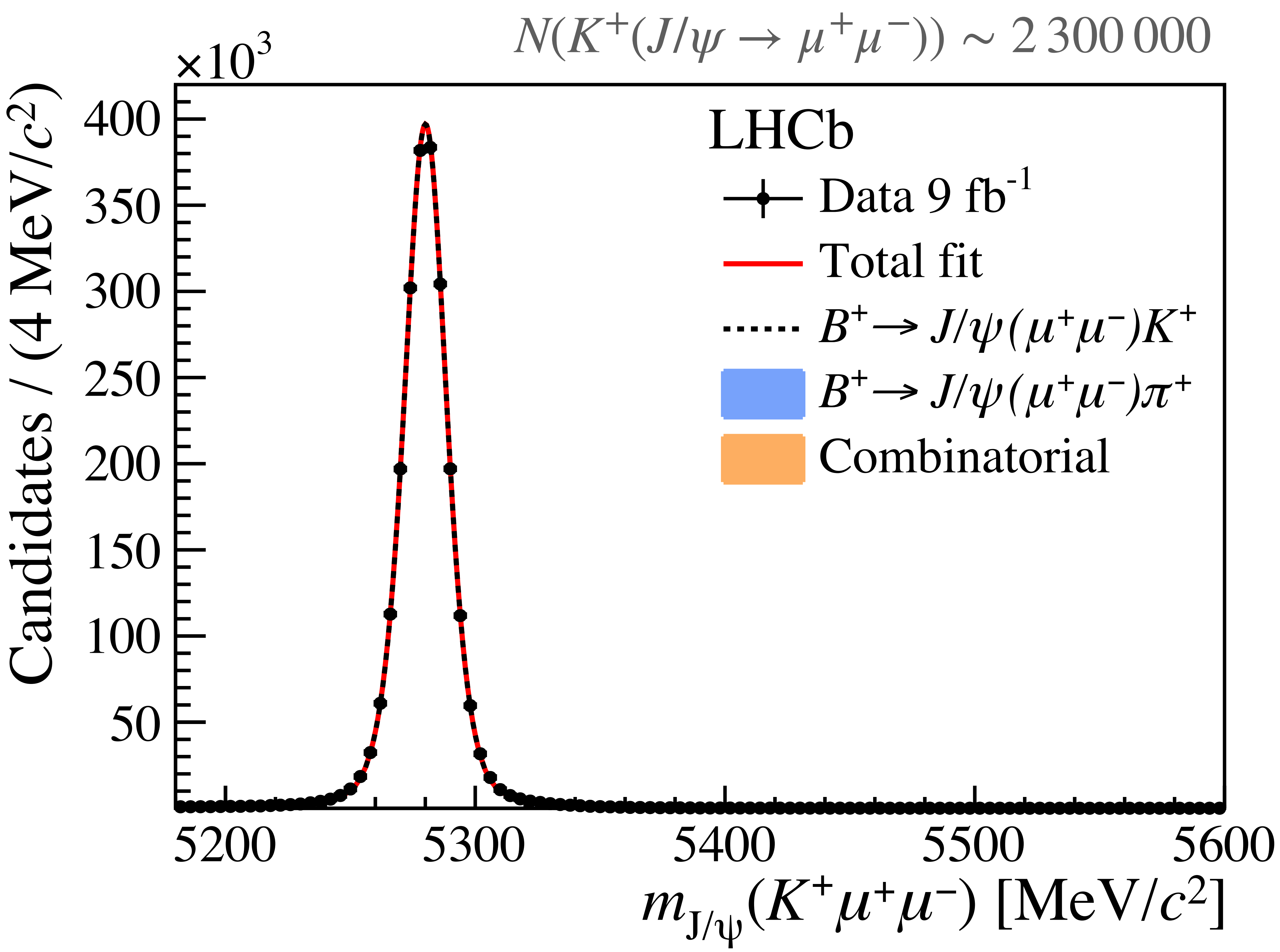

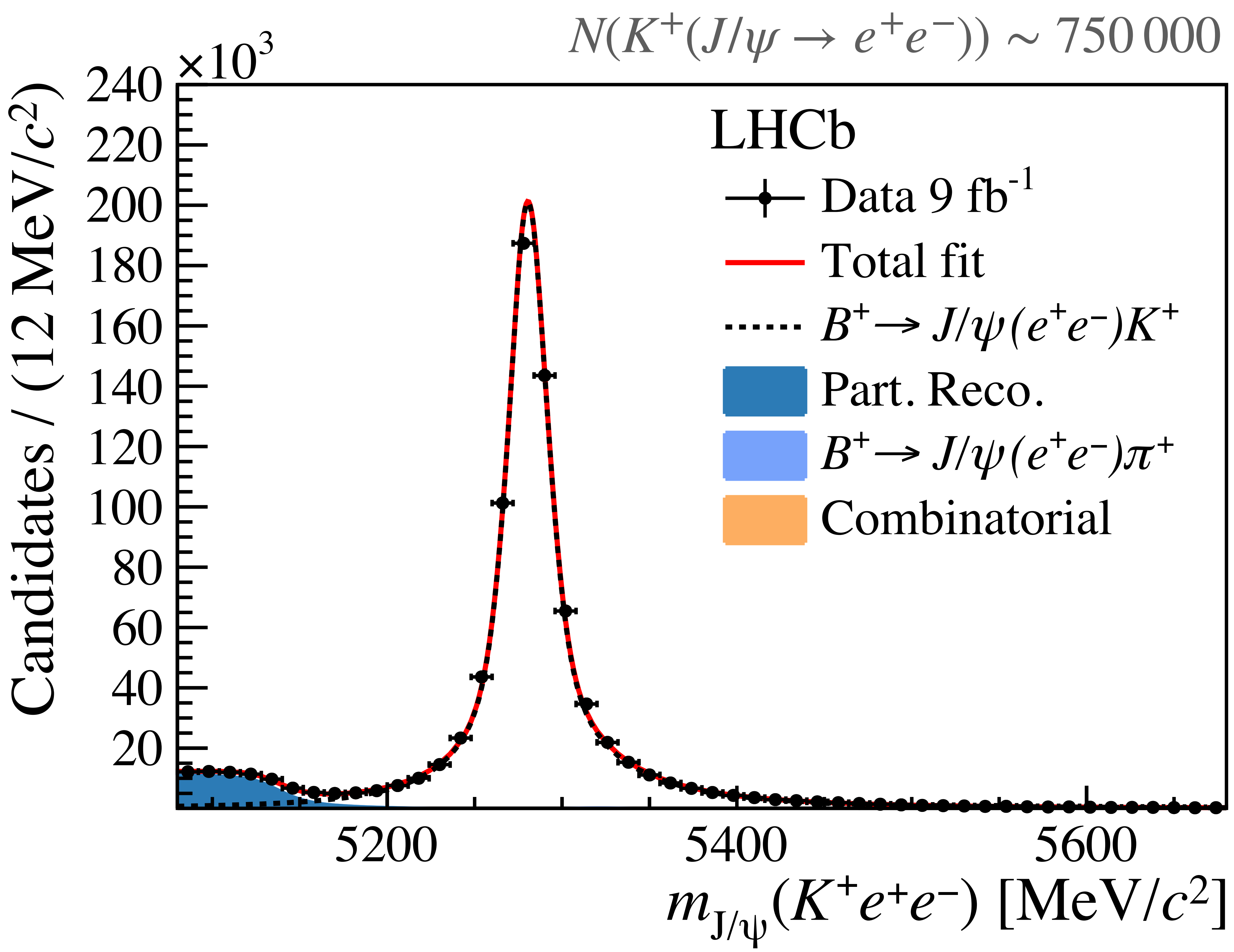

- High statistics of the control modes, not all of the backgrounds are visible in the plots
- Resolution on reconstructed B^+ mass improved by constraining dilepton invariant mass to that of J/ψ

Efficiency calibration

Efficiencies are estimated from simulated samples and calibrated using data, following identical procedure as in the previous analysis:

- Particle identification efficiency calibration;
- Trigger efficiency;
- Calibration of B^+ kinematics;
- Resolution of q^2 and of reconstructed B^+ mass;

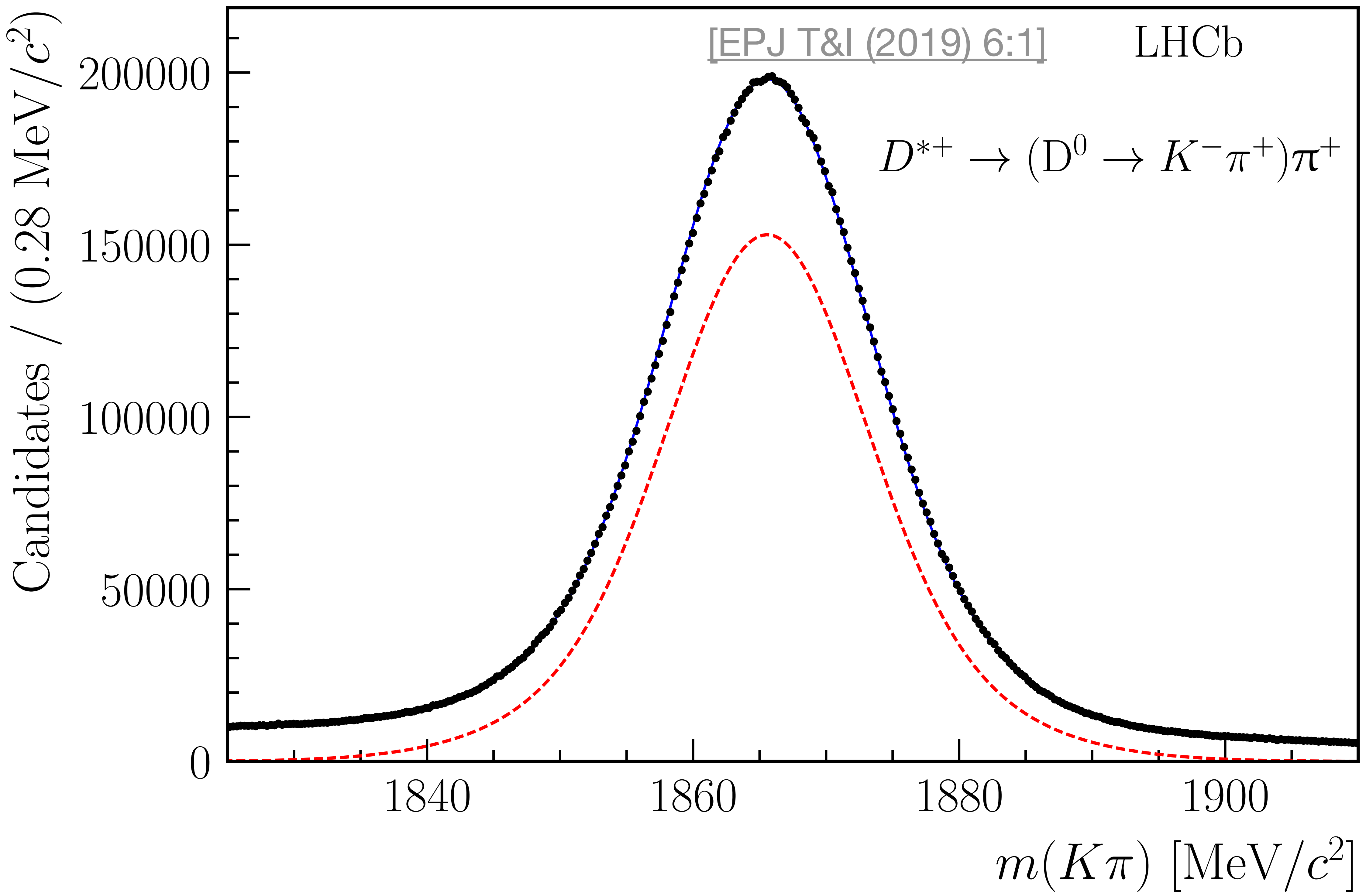

Fit to the data sample used as a source of $\pi^{\pm}$ and $K^{\pm}$ calibration

Efficiency calibration

Efficiencies are estimated from simulated samples and calibrated using data, following identical procedure as in the previous analysis:

- Particle identification efficiency calibration;
- Trigger efficiency;
- Calibration of B^+ kinematics;
- Resolution of q^2 and of reconstructed B^+ mass;

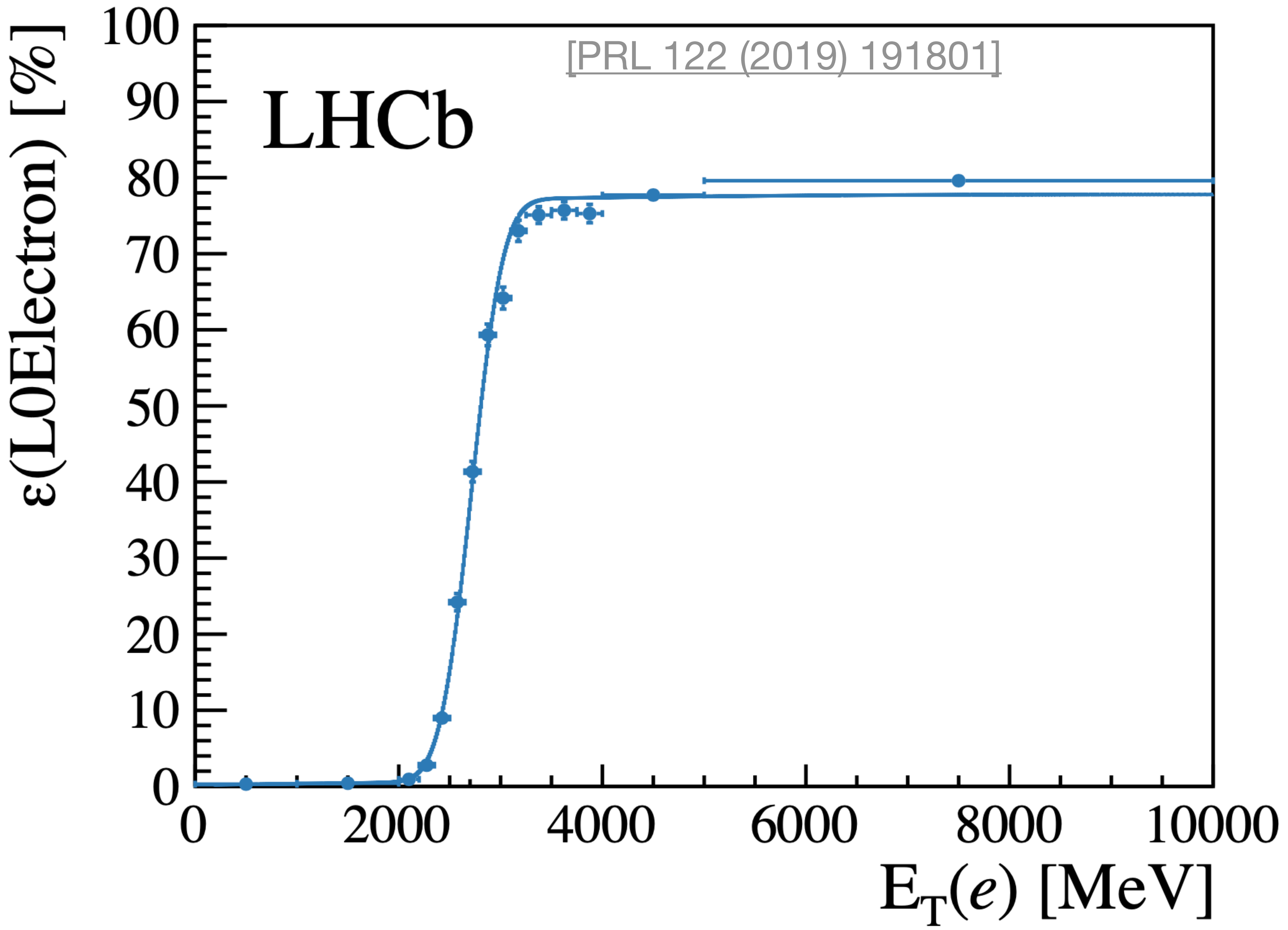

Measurement of the electron trigger efficiency using $B^+ \to K^+ J/\psi(ee)$ data

Efficiency calibration

Efficiencies are estimated from simulated samples and calibrated using data, following identical procedure as in the previous analysis:

- Particle identification efficiency calibration;
- Trigger efficiency;
- Calibration of B^+ kinematics;
- Resolution of q^2 and of reconstructed B^+ mass;

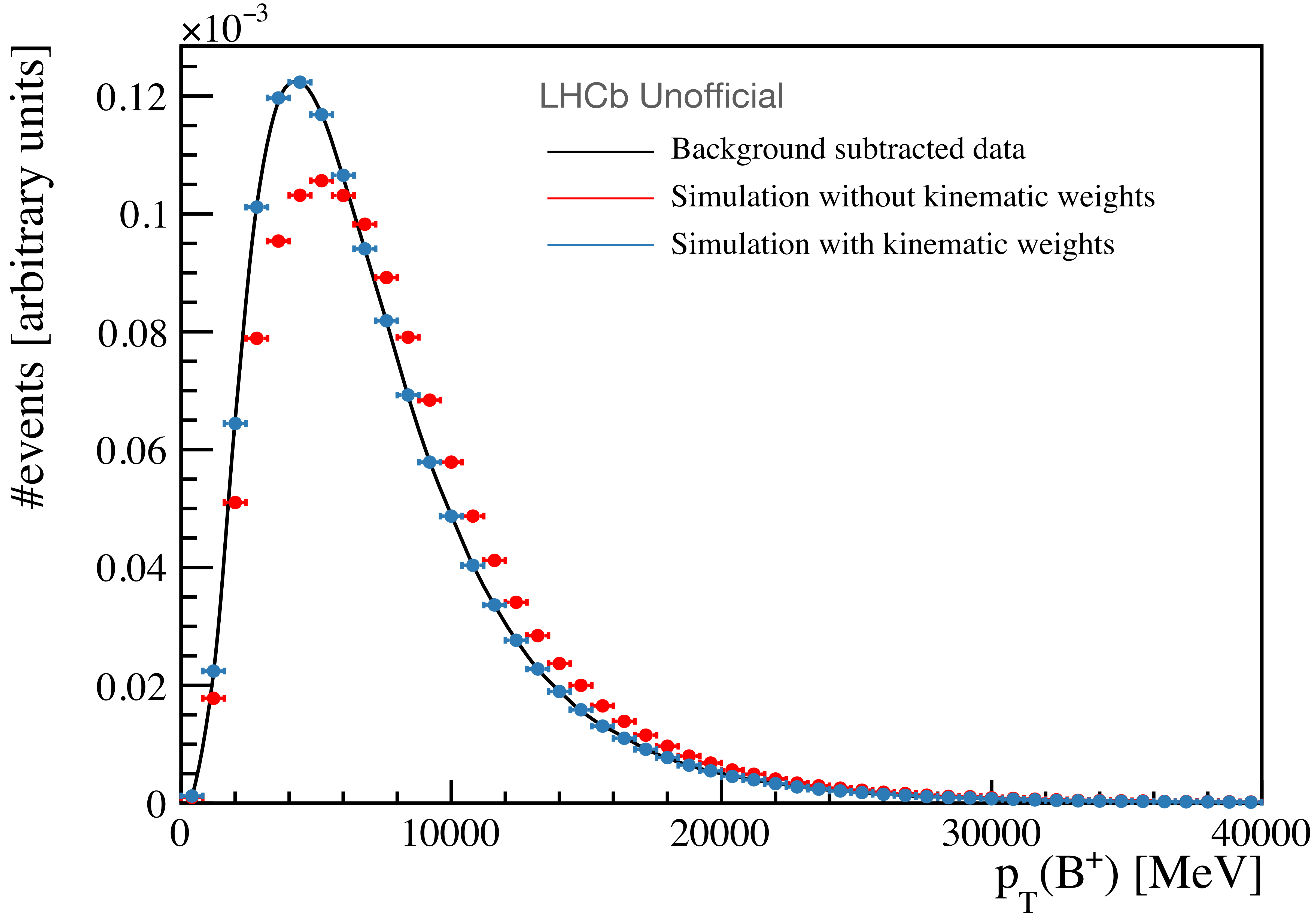

Transverse momentum spectrum of $B^+ \to K^+ J/\psi(\mu\mu)$ calibration data vs simulation

Efficiency calibration

Efficiencies are estimated from simulated samples and calibrated using data, following identical procedure as in the previous analysis:

- Particle identification efficiency calibration;
- Trigger efficiency;
- Calibration of B^+ kinematics;
- Resolution of q^2 and of reconstructed B^+ mass;

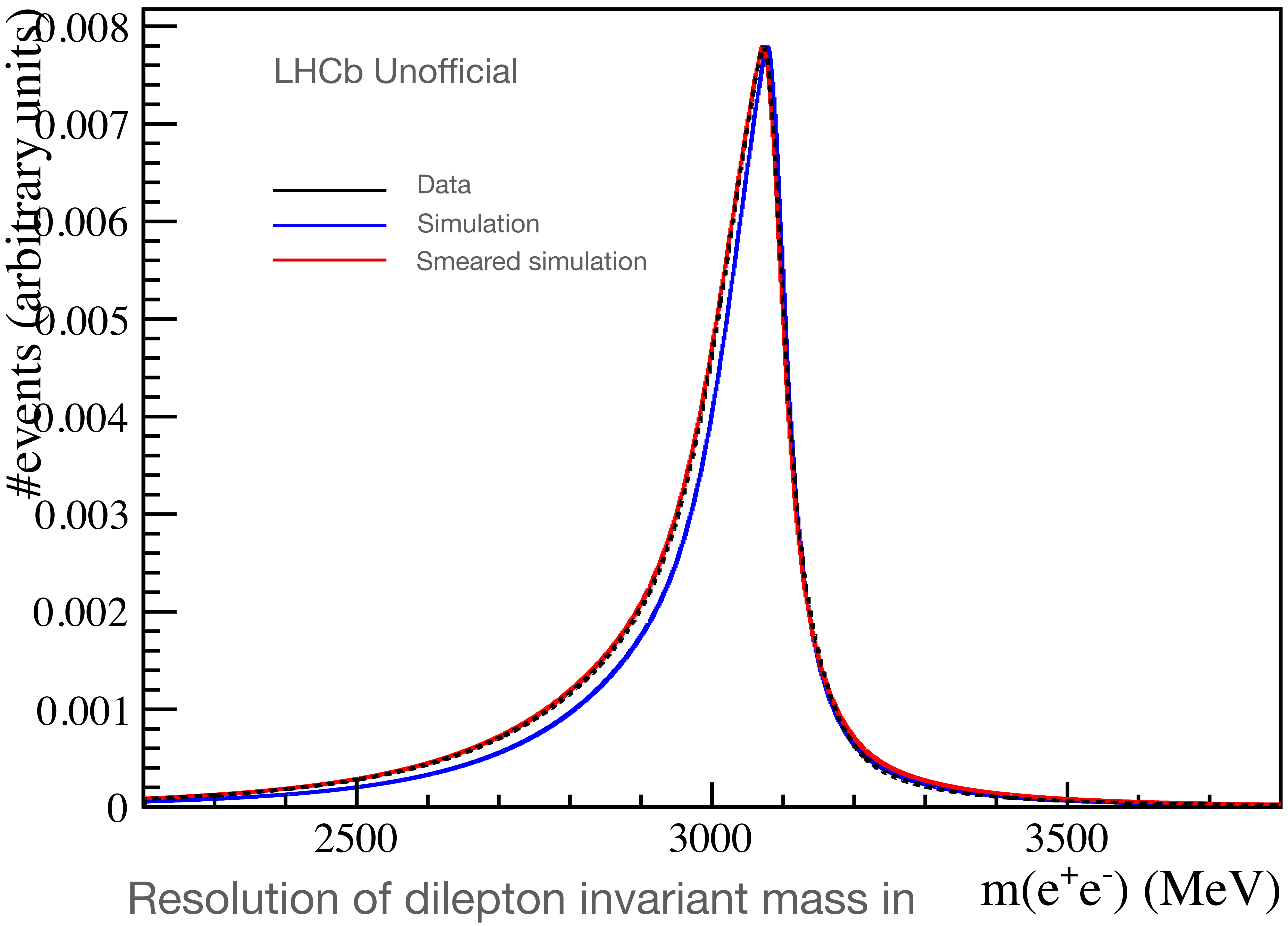

Resolution of dilepton invariant mass in $B^+ \to K^+ J/\psi(ee)$ calibration data vs simulation

Efficiency calibration

Efficiencies are estimated from simulated samples and calibrated using data, following identical procedure as in the previous analysis:

- Particle identification efficiency calibration;
- Trigger efficiency;
- Calibration of B^+ kinematics;
- Resolution of q^2 and of reconstructed B^+ mass;

Leads to excellent agreement between data and simulation

- Extensive cross checks to verify procedure

[PRL 122 (2019) 191801]

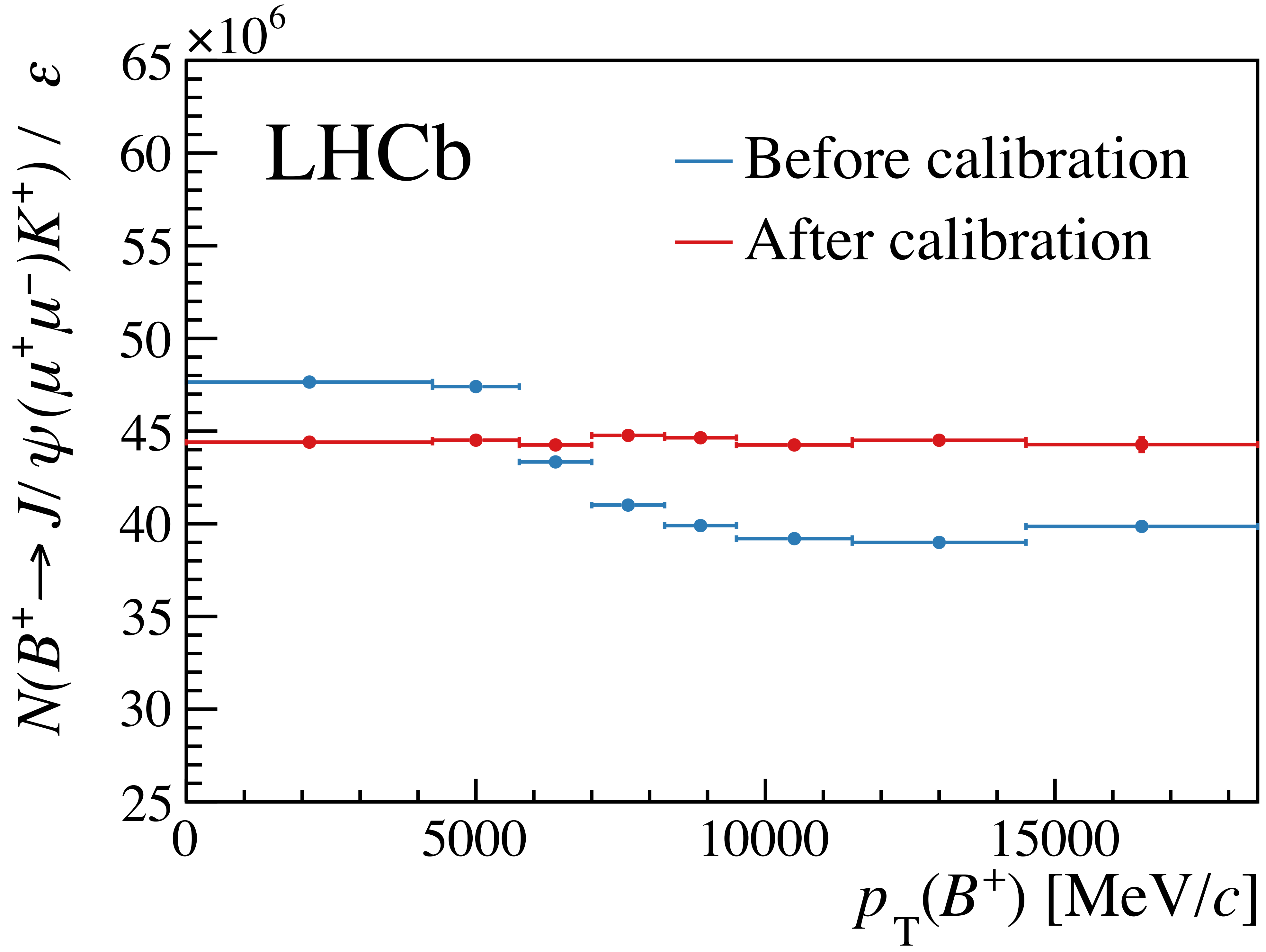

Cross check: $r_{J/\psi}$ single ratio

$$r_{J/\psi} = \frac{N(K^+ J/\psi(\mu\mu))}{N(K^+ J/\psi(ee))} \boxed{\frac{\varepsilon(K^+ J/\psi(ee))}{\varepsilon(K^+ J/\psi(\mu\mu))}}$$

- Single ratio requires direct control of electrons with respect to muons:
  - Stringent cross-check of efficiencies.

Measured value $\boxed{r_{J/\psi} = 0.981 \pm 0.020 \text{ (stat \& syst)}}$

Cross check: $r_{J/\psi}$ single ratio

[arXiv:2103.11769]

$$r_{J/\psi} = \frac{N(K^+ J/\psi(\mu\mu))}{N(K^+ J/\psi(ee))} \boxed{\frac{\varepsilon(K^+ J/\psi(ee))}{\varepsilon(K^+ J/\psi(\mu\mu))}}$$

- Single ratio requires direct control of electrons with respect to muons
  - Stringent cross-check of efficiencies

Measured value: $\boxed{r_{J/\psi} = 0.981 \pm 0.020 \text{ (stat \& syst)}}$

- Cross check that efficiencies are understood in all kinematic regions by checking $r_{J/\psi}$ is flat in all variables relevant to the detector response.
  - If deviations from flatness is actually due to efficiency mismodelling, impact on R_K is of 0.1%.

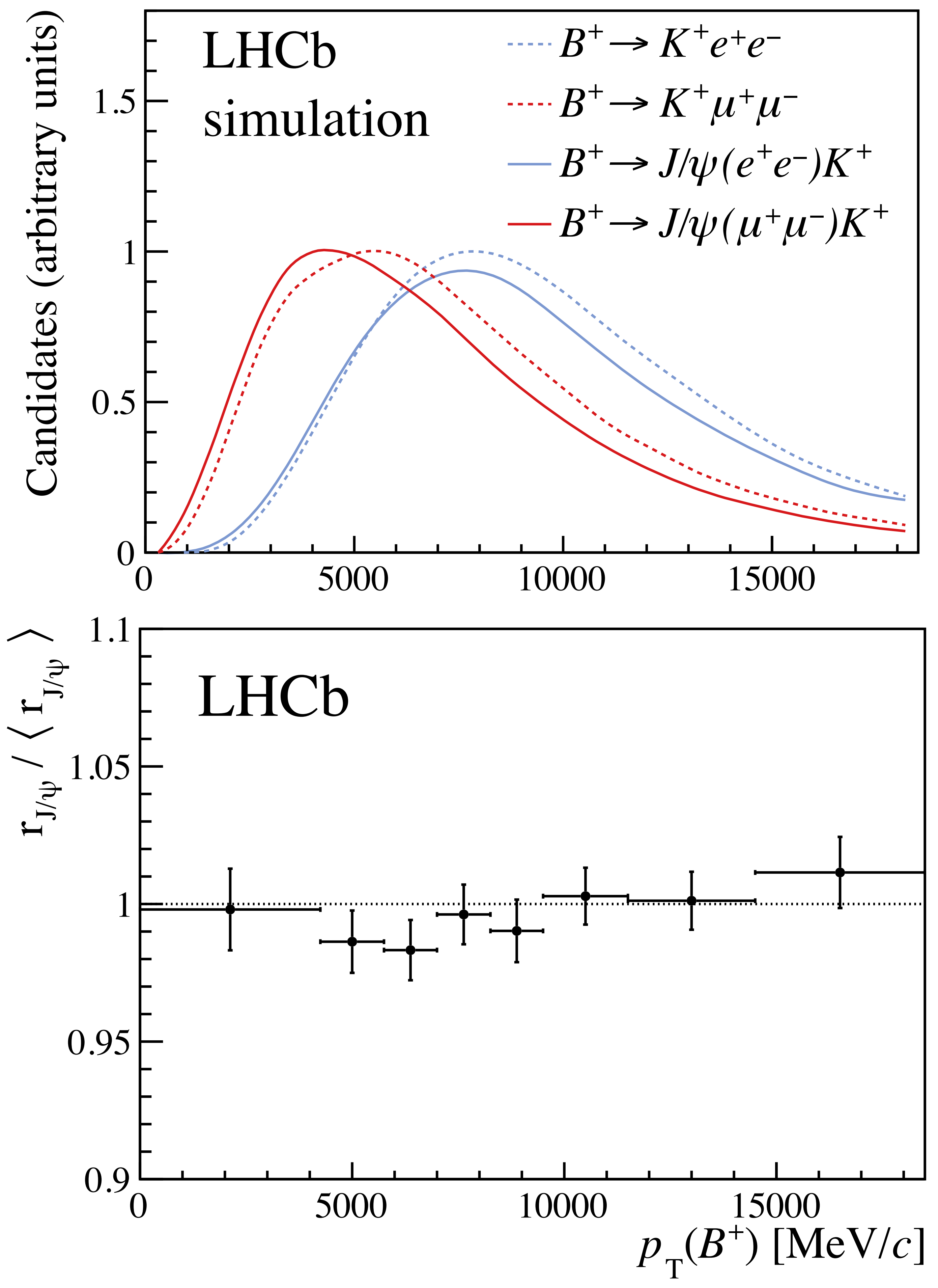

Cross check: $r_{J/\psi}$ single ratio

[arXiv:2103.11769]

$$r_{J/\psi} = \frac{N(K^+ J/\psi(\mu\mu))}{N(K^+ J/\psi(ee))} \boxed{\frac{\varepsilon(K^+ J/\psi(ee))}{\varepsilon(K^+ J/\psi(\mu\mu))}}$$

- Single ratio requires direct control of electrons with respect to muons
    - Stringent cross-check of efficiencies

Measured value: $\boxed{r_{J/\psi} = 0.981 \pm 0.020 \text{ (stat \& syst)}}$

- Cross check that efficiencies are understood in all kinematic regions by checking $r_{J/\psi}$ is flat in all variables relevant to the detector response.
    - If deviations from flatness is actually due to efficiency mismodelling, impact on R_K is of 0.1%.
    - Check is also performed in 2D

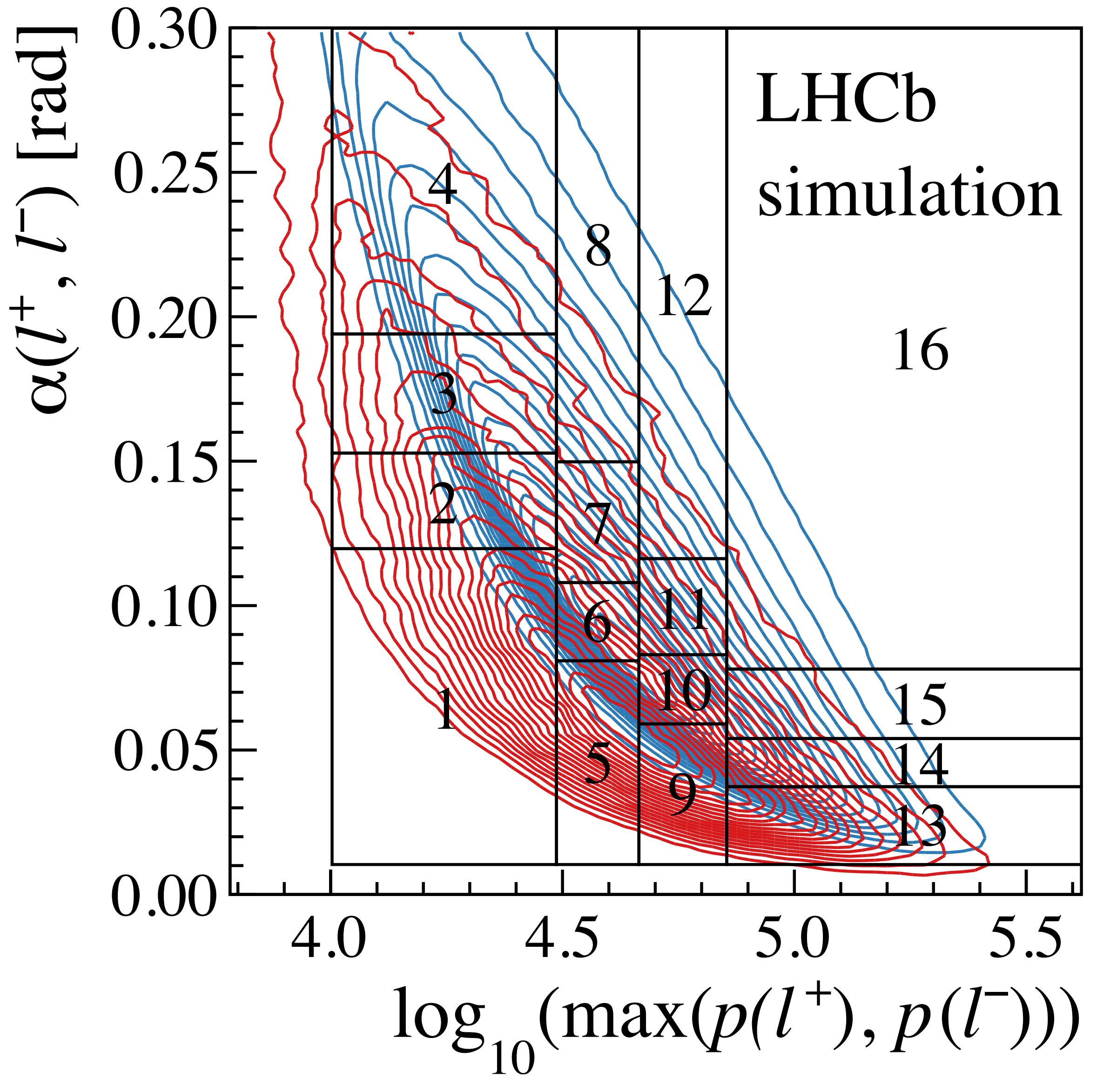

$B^+ \to K^+ J/\psi(e^+e^-)$ and $B^+ \to K^+(e^+e^-)$ distributions

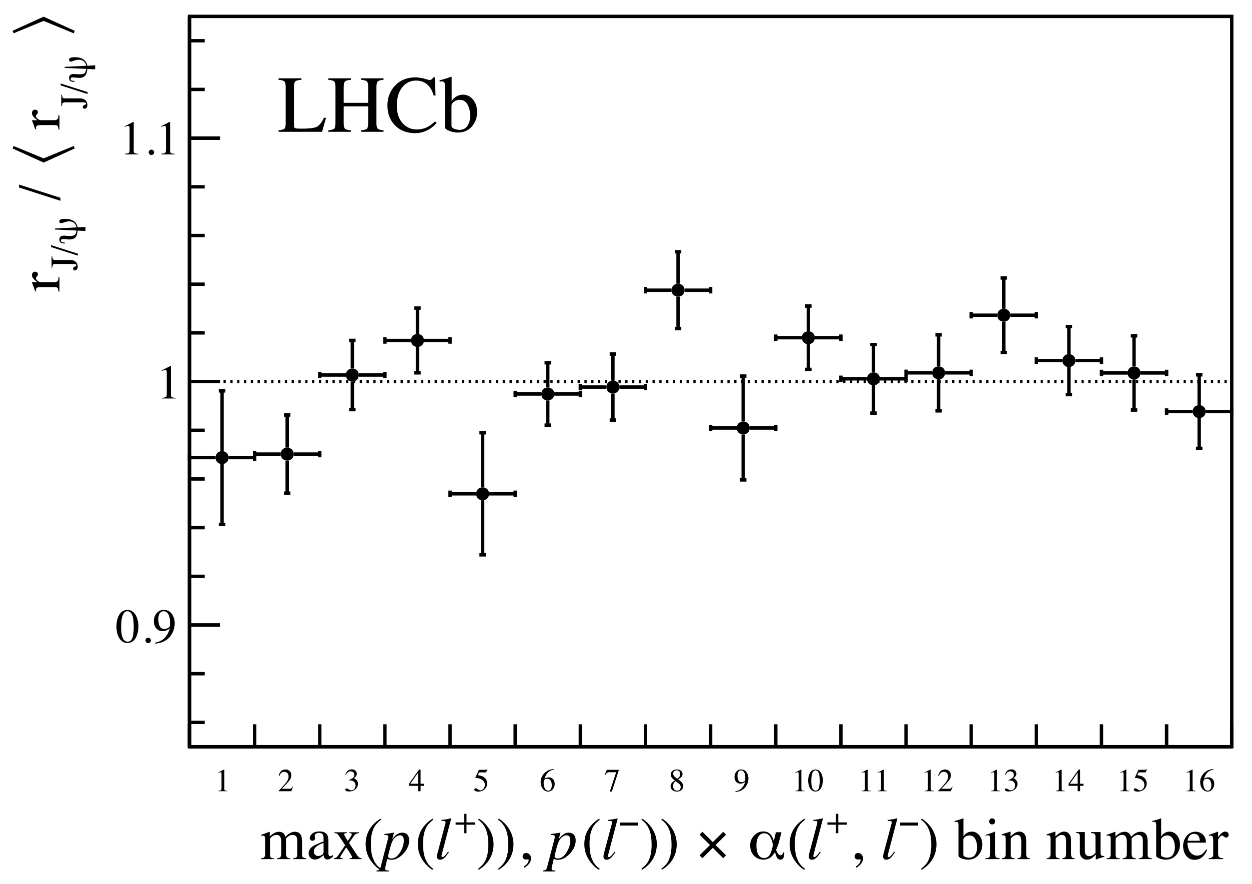

Cross check: $R_{\psi(2S)}$ double ratio

$$R_{\psi(2S)} = \frac{\mathcal{B}(B^+ \to K^+\psi(2S)(\mu\mu))}{\mathcal{B}(B^+ \to K^+\psi(2S)(ee))} \Bigg/ \frac{\mathcal{B}(B^+ \to K^+J/\psi(\mu\mu))}{\mathcal{B}(B^+ \to K^+J/\psi(ee))}$$

- Data are selected at the $\psi(2S)$ resonance with a suitable q^2 cut.
- Independent validation of double-ratio procedure.
- Test of the efficiencies at q^2 away from J/ψ.

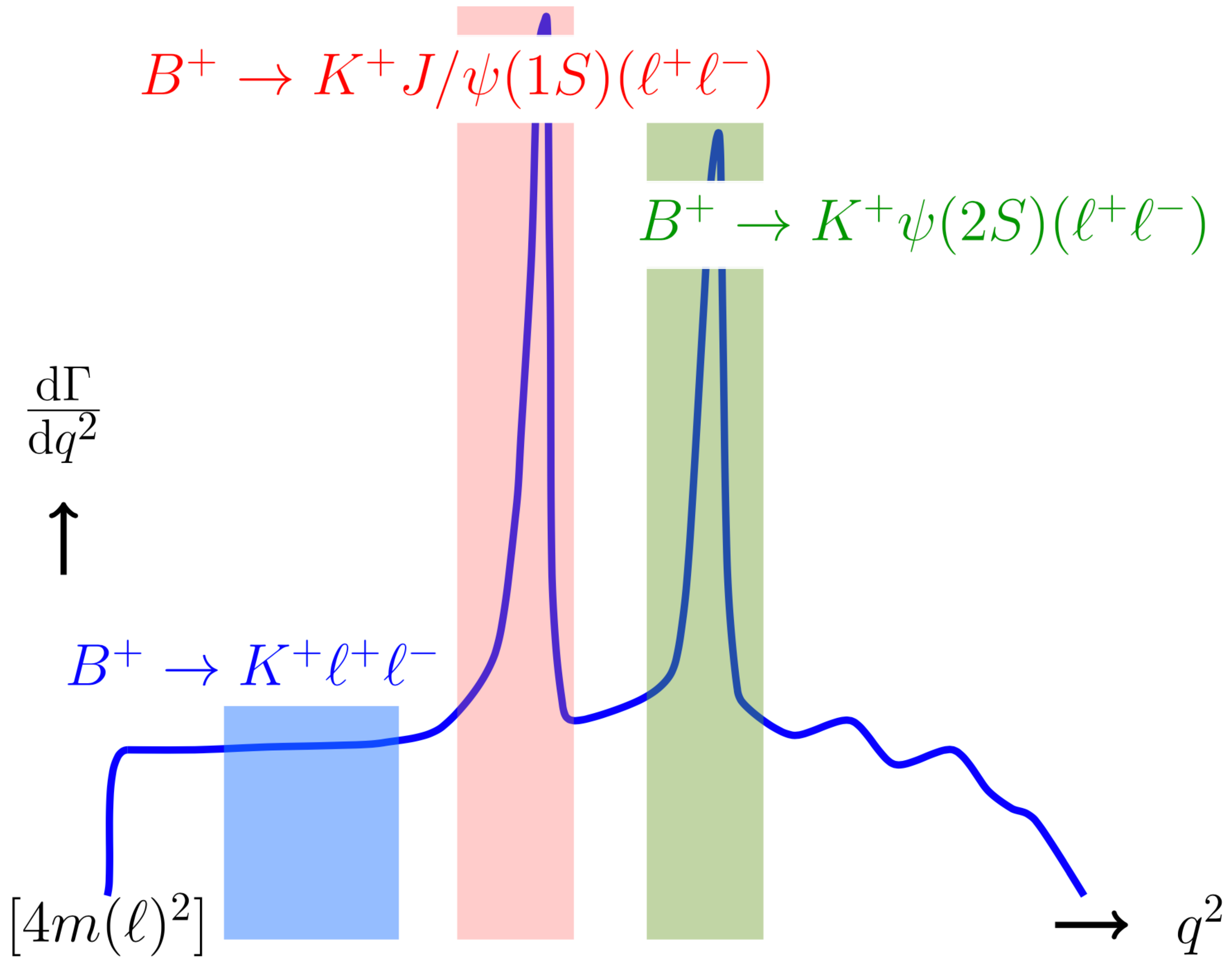

Cross check: $R_{\psi(2S)}$ double ratio

[arXiv:2103.11769]

$$R_{\psi(2S)} = \frac{\mathcal{B}(B^+ \to K^+\psi(2S)(\mu\mu))}{\mathcal{B}(B^+ \to K^+\psi(2S)(ee))} \Bigg/ \frac{\mathcal{B}(B^+ \to K^+J/\psi(\mu\mu))}{\mathcal{B}(B^+ \to K^+J/\psi(ee))}$$

- Data are selected at the $\psi(2S)$ resonance with a suitable q^2 cut.
- Independent validation of double-ratio procedure.
- Test of the efficiencies at q^2 away from J/ψ.
- Result is well compatible with unity:

Measured value $\boxed{R_{\psi(2S)} = 0.997 \pm 0.011 \text{ (stat \& syst)}}$

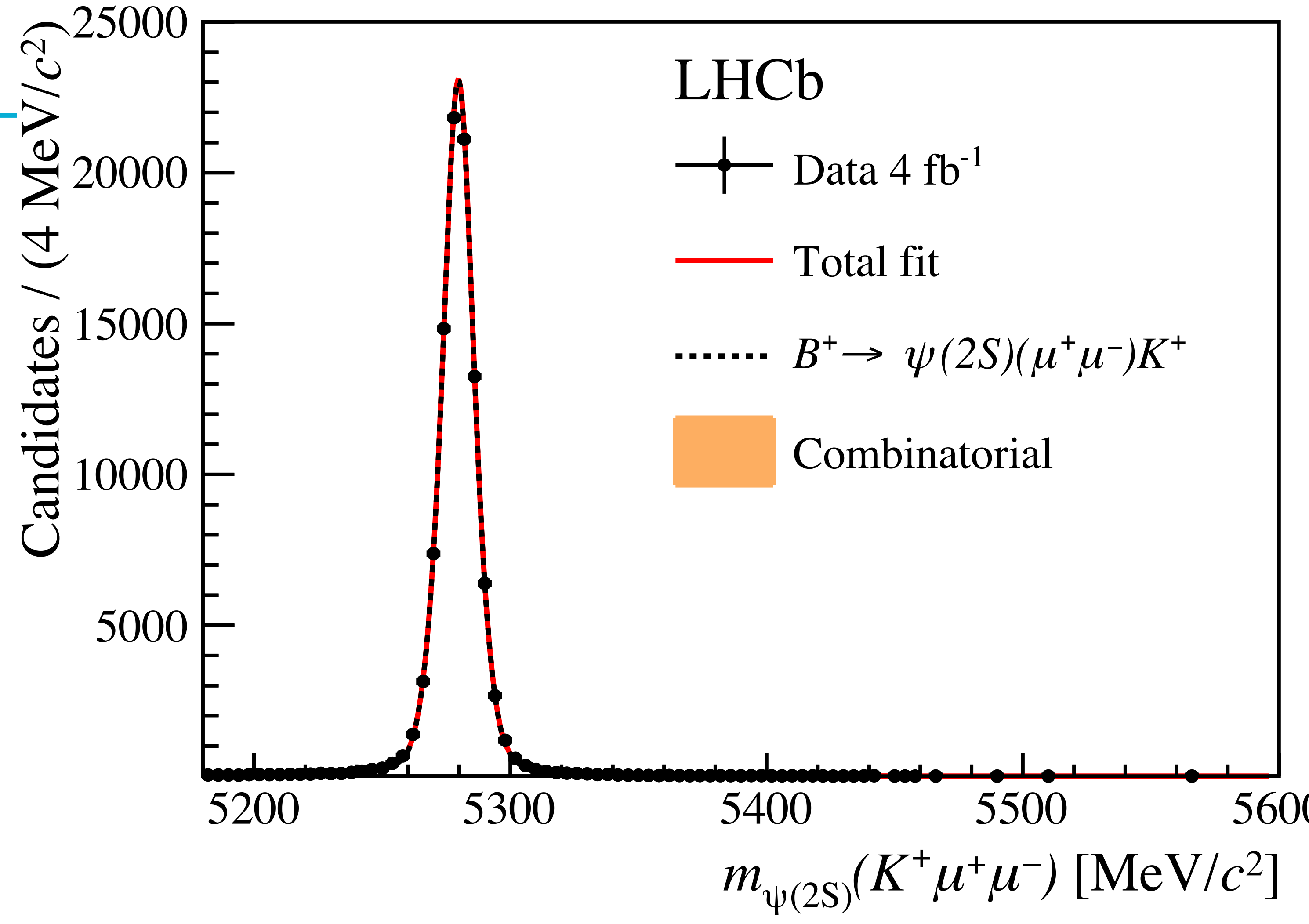

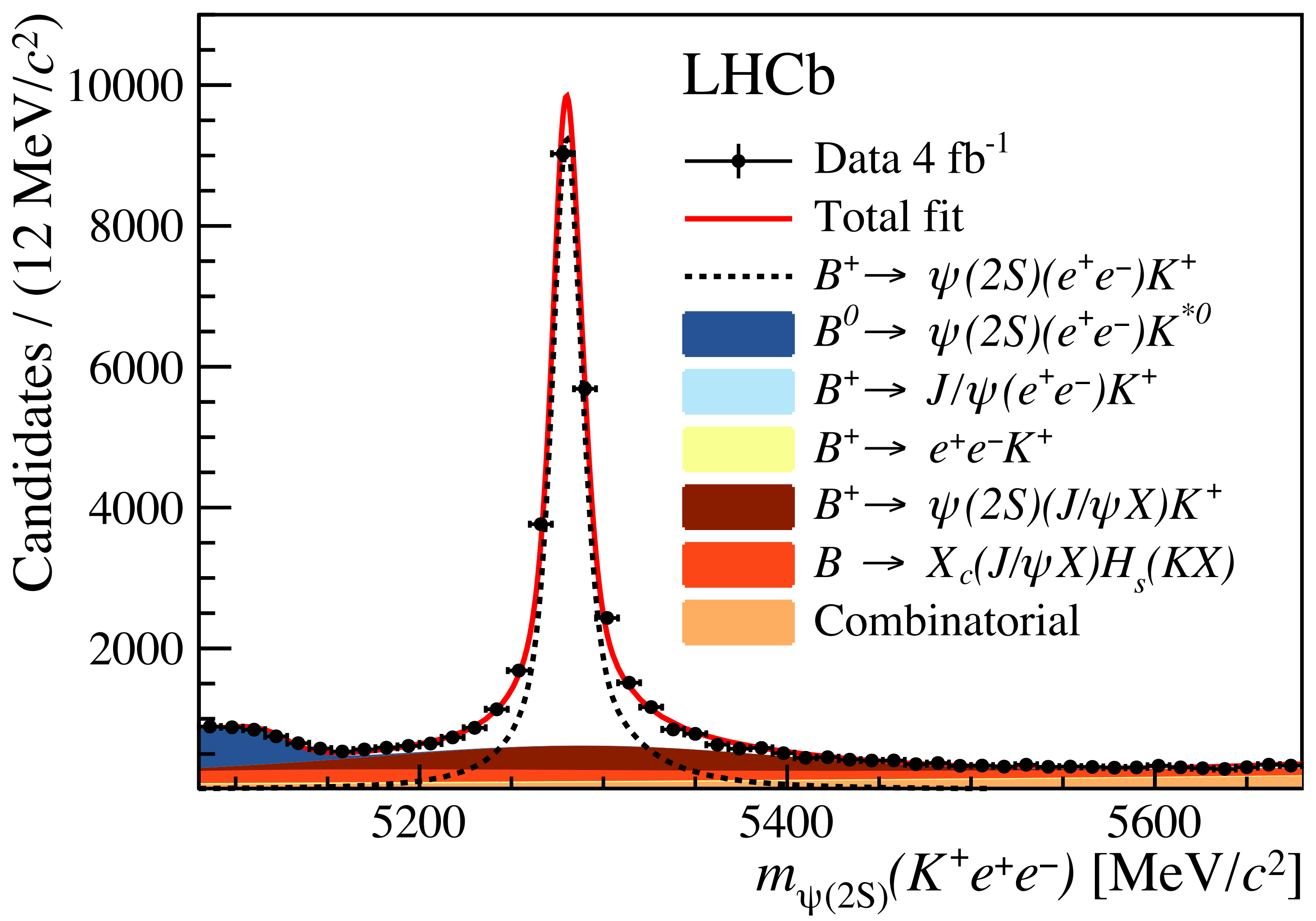

Dilepton mass constrained to mass of $\psi(2S)$